Adaptive quantized control for uncertain networked systems

Nikolaos Moustakis

Master of Science Thesis

TU Delft Delft University of Technology

Delft Center for Systems and Control

Adaptive quantized control for uncertain networked systems

Master of Science Thesis

For the degree of Master of Science in Systems and Control at Delft University of Technology

Nikolaos Moustakis

June 22, 2017

Faculty of Mechanical, Maritime and Materials Engineering (3mE) · Delft University of Technology

Delft University of Technology
Department of
Delft Center for Systems and Control (dcsc)

The undersigned hereby certify that they have read and recommend to the Faculty of Mechanical, Maritime and Materials Engineering (3mE) for acceptance a thesis entitled

Adaptive quantized control for uncertain networked systems

by

Nikolaos Moustakis

in partial fulfillment of the requirements for the degree of

Master of Science Systems and Control

Dated: June 22, 2017

Supervisor(s):

Dr. S. Baldi

Mr. S. Yuan

Reader(s):

Dr. T. Keviczky

Dr. R.V. Prasad

Dr. R. Ferrari

Abstract

Major advancements over the last few decades in communication networks gave rise to the new paradigm of Networked Control Systems (NCSs). Within this paradigm, sensing and actuation signals are exchanged among various parts of a single system or among many subsystems via communication networks. Although this enables one to perform more complex tasks than traditional control paradigms, it comes at the cost of complicating the design phase and the required analysis tools. One of the major challenges when considering a network is quantization effect which affects the performance of any control laws that were designed without taking the network effects into account.

Even if the NCS paradigm is well established, few works are available on adaptive methods for NCSs: this MSc thesis establishes novel adaptive control approaches that attain asymptotic tracking for linear systems and switched linear systems with parametric uncertainties, when input measurements are quantized due to the presence of a communication network closing the control loop. In addition to enlarging the class of systems for which the adaptive quantized control can be solved, a hybrid control policy is applied to a novel dynamic quantizer with dynamic offset to address the tracking problem.

The MSc thesis is split into two parts: in the first part we consider the model reference adaptive control of a linear uncertain system, where a Lyapunov-based approach is used to derive the adaptive adjustments for the dynamic range, the dynamic offset and the control parameters. In the second part, the approach is extended to switched uncertain linear systems with dwell-time switching, where a new time-varying Lyapunov-like function is adopted: it is proven analytically that the new Lyapunov function we introduce, overcomes the need for zooming-out at every time instant in order to compensate the possible increment of the Lyapunov function.

The proposed quantized adaptive control schemes are applied to two benchmark examples: an electro-hydraulic system and the piecewise linear model of the NASA GTM aircraft, respectively.

List of Figures

Contents

List of Notation

The notations used in the MSc thesis are standard:

$\mathbb{N}^+$: the set of non-negative integers;

$\mathbb{R}_0^+$: the set of non-negative real numbers including zero;

$\lambda_{max}(X)$, $(\lambda_{min}(X))$: the largest (smallest) eigenvalue of matrix X;

$\|X\| = \sqrt{\lambda_{max}(XX^T)}$: the induced 2-norm of matrix X. The superscript T represents the transpose of matrix X;

$\|x\| = \sqrt{\sum_{i=1}^{n}|x_i|^2}$: the Euclidean norm of a vector $x \in \mathbb{R}^n$;

$tr[X]$: the trace of a square matrix X;

$\mathscr{L}_\infty$ class: a vector signal $x \in \mathbb{R}^n$ is said to belong to $\mathscr{L}_\infty$ class ($x \in \mathscr{L}_\infty$), if $\max_{t\geq 0}\|x(t)\| < \infty$, $\forall t \geq 0$.

Acknowledgment

This MSc thesis concludes my work as a MSc student in Delft University of Technology and signs the end of two exciting years. I would like to take this chance in order to thank all the DCSC community for providing a stimulating environment and for keeping the motivation of MSc students high.

I would like to express my gratitude to my supervisors, dr. Simone Baldi and mr. Shuai Yuan, for giving me the opportunity to work in such interesting and promising research topics. I would also like to thank them for their continuous support and guidance and for always keeping the research project challenging and me motivated.

I would also like to express my gratitude to my friends here, in the Netherlands, for the amazing time we had all these years and for their continuous support during my thesis. I extend my deepest gratitude to my family, for their unconditional love and trust.

Finally, I would like to thank everyone that directly or indirectly helped me in their own way during my thesis.

"Differences of habit and language are nothing at all if our aims are identical and our hearts are open."

— *Albus Dumbledore,'Harry Potter and the Goblet of Fire'*

Chapter 1

Introduction

With its clearly defined goal of designing control systems that can adapt to parametric uncertainties and changing conditions, adaptive control constitutes a flourishing research area within the control and systems society [4], [5], providing significant advantages in several application domains [6], [7], [8], [9].

Although the research field of networked control systems is emerging rapidly, only limited attention has been devoted to adaptive tracking with network-induced constraints. This chapter introduces the problem of quantization in the tracking control problem and is organized as follows: Section 1-1 presents the phenomenon of quantization and shows the challenges imposed by quantization in the performance of control laws, which were designed ideally in the absence of networks. Section 1-2 presents the state of art methodologies that have been proposed by the research community to address the tracking problem, using quantized measurements. Section 1-3 concludes this introductory chapter, stating the research questions we aim to tackle through this MSc thesis.

1-1 Control with quantization constraints

A networked control system (NCS) is a control system wherein the control loops are closed through a communication network [10], [11], [12]. A schematic representation of a NCS is shown in Fig. 1-1. Because of the network, control and feedback signals exchanged among the system's components must be quantized.

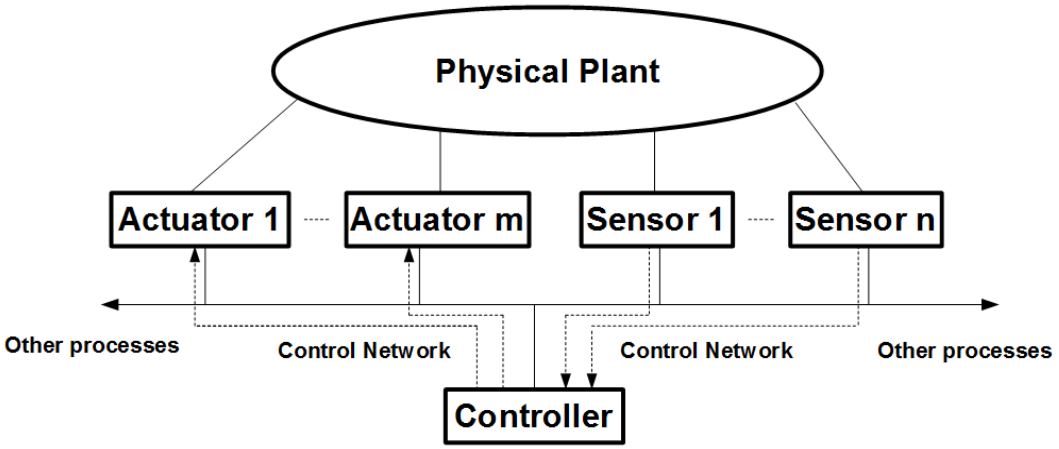

Figure 1-1: Typical architecture of an NCS [1]

A quantizer is a device that converts a real-valued signal into a piecewise constant one taking a finite set of values. In the literature it is usually assumed that the quantization regions are rectilinear and are either of equal size (*uniform quantizer*) or get smaller close to the origin (*logarithmic quantizer*). The most common types of quantizers are depicted in Fig. 1-2.

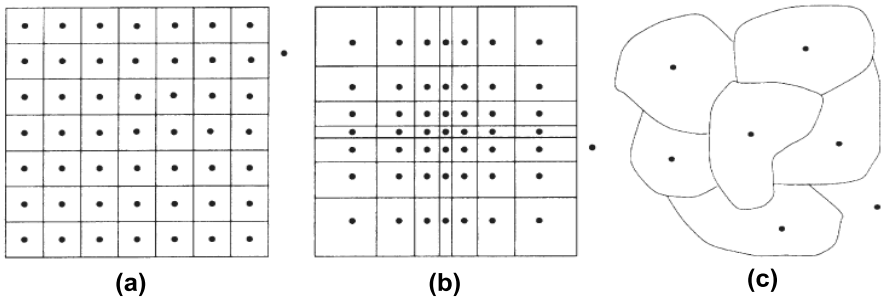

Figure 1-2: Quantization regions: (a) uniform, (b) logarithmic, (c) general [2]

The complement of the union of all quantization regions of finite sizes is the infinite quantization region, in which the quantizer saturates (the corresponding value is shown in Fig. 1-2 with the extra dot outside the quantization region). Let $u \in \mathbb{R}^q$ be the variable being quantized. The uniform static quantizer is described by a function $g : \mathbb{R} \to Q$, where $Q \subset \mathbb{R}^q$. The finite set of values is defined $\{u \in \mathbb{R}^q : g(u) = i\}$, $i \in Q$.

There are two phenomena that account for changes in the system's behavior caused by quantization. The first one is *saturation*: if the quantized signal is outside the range of the quantizer, then the quantization error can be in principle large, and the control law designed for the ideal case of no quantization leads to instability. The second phenomenon resulting from quantized signals is the *deterioration of performance* near the equilibrium points: as the difference between the current and the desired values of the signal to be quantized become small, higher precision is required, and as a result, in the presence of quantization errors asymptotic convergence is in general impossible.

To illustrate more precisely what is meant by saturation we assume that positive real numbers M and Δ exist such that the two following conditions hold:

Condition 1. If

$$\|u\| \leq M \tag{1-1}$$

then

$$\|g(u) - u\| \leq \Delta. \tag{1-2}$$

Condition 2. If

$$\|u\| > M \tag{1-3}$$

then

$$\|g(u)\| > M - \Delta. \tag{1-4}$$

Condition 1 gives a bound on the quantization error when the quantizer does not saturate. Condition 2 provides a way to detect the possibility of saturation. We will refer to M and Δ as the *quantization range* and *quantization error* respectively. Given the maximal size of finite quantization regions and the size of these regions, suitable values for M and Δ can be obtained. Furthermore, given the number of quantization regions, we can define a bit sequence corresponding to each quantization level. The idea is illustrated graphically in Fig. 1-3.

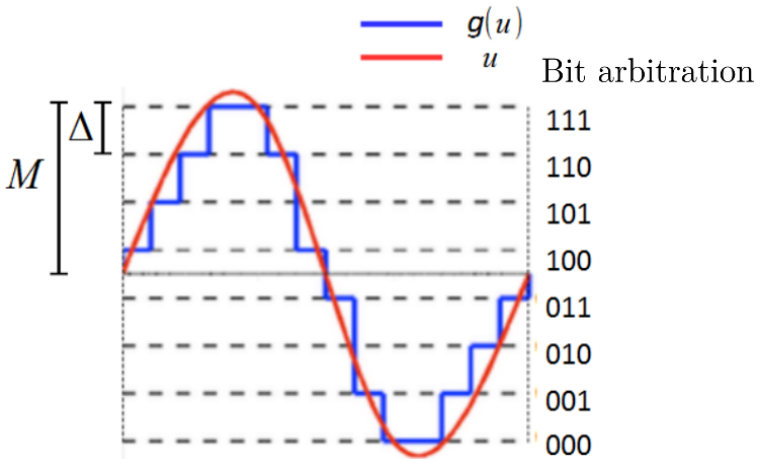

Figure 1-3: Original and quantized signal (red line corresponds to continuous signal, blue line corresponds to quantized signal)

1-2 State of the art

Much attention has been devoted by the control community to asymptotic stability in non-adaptive NCSs in the presence of quantization, with a focus on regulation problems. The most established research approaches for achieving asymptotic regulation rely on a hybrid control approach with dynamic quantization mechanisms such as the one referred to as "zooming" [13], [14], [15]. This mechanism takes its name from the analogy with the zooming mechanism in digital cameras: since the quantizer has a fixed number of quantization levels (i.e number of pixels), when the state is outside its range region, the quantizer "zooms out" so that the state can be captured within the region. This can be achieved by increasing the size of the range. On the other hand, once the state comes close to the origin, we can "zoom in" by reducing the

size of the range so that the quantization resolution becomes finer while the region becomes smaller. The idea is illustrated graphically in Fig. 1-4. Repeating this zooming-in, we can obtain asymptotic stabilization.

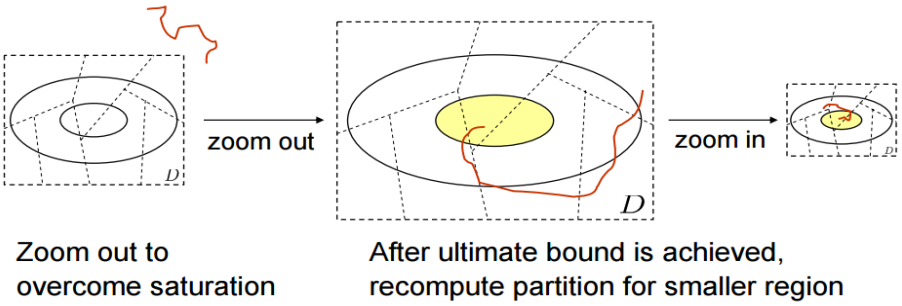

Figure 1-4: Dynamic quantization ("zooming") mechanism [3]

The research on adaptive NCSs with quantization is not as developed as its non-adaptive counterpart, and most of this research is also limited to regulation problems. Recently, [16] considered a passification-based adaptive controller with quantized measurements and disturbances, where ultimate boundedness can be obtained. The authors in [17] developed a direct adaptive control framework with a logarithmic quantizer, guaranteeing partial asymptotic stability, i.e. Lyapunov stability of the closed-loop system states and attraction with respect to a guaranteed ultimate bound. For nonlinear uncertain systems, [18], [19], developed direct adaptive control schemes with guaranteed global ultimate boundedness: this is due to the use of logarithmic quantizers with deadzone around zero control input. The reason for the focus on regulation problems might be explained with the fact that the quantizer is typically anti-symmetric with respect to the origin which prevents from achieving high precision in the tracking case. A smart solution has been recently proposed in [20], [21], where asymptotic tracking has been achieved via a sliding mode approach. It has to be recognized however, that the implementation of a sliding-mode controller which has to send information infinitely often in an NCS is not at all straightforward.

Less attention has been devoted by research community to the adaptive control of switched systems with quantized measurements. Switched systems are used to model many complex systems exhibiting an interaction between continuous and discrete dynamics. Such systems, commonly referred to as hybrid systems, include multi-agent systems [22], automobile power trains [23], traffic light controls [24], power converters [25], fault tolerant systems [26], [27] and many more. In recent decades many efforts have been increasingly devoted to studying switched systems, mainly stability and stabilization problems [26], [28], [29]. Most recently, advanced robust and adaptive control methodologies have been developed for complex systems like uncertain switched systems, cf. [30], [31], [32] for robust control, and [33], [34], [35], [36], [37] for adaptive control. Extensions to (non-adaptive) switched systems into a NCS framework with quantized measurements have been studied. The authors in [38] designed a dynamic quantizer and a switching law with average dwell time to stabilize switched linear systems using quantized output-feedback measurements; in [39] a switching law was proposed based on average dwell time and a dynamic quantizer to stabilize a sample-data switched linear system considering asynchronous switching between system modes and controller modes; the authors in [40] consider the fault detection problem for switched systems with quantization effects; [41] studied the problem of stabilizing switched linear systems with

output feedback controllers based on a common Lyapunov function considering switching delays between system modes and controller modes.

1-3 Research questions

From this overview of the state of the art, we can see that most results on NCSs, with an eye on adaptive control and in the presence of quantization, focus on uncertain non-switched systems. As a result, the adaptive control of switched systems with quantized measurements is a completely open and relevant problem which motivates our research. The research questions we aim to tackle throughout this MSc thesis are presented as follows:

- Address large uncertainty in the unknown system parameters;
- Achieve asymptotic tracking in the quantized control setting without sending information infinitely often;
- Enlarge the class of quantized adaptive tracking control to include uncertain switched linear systems;
- Avoid the quantizer to zoom out at every switching instants in order to compensate for discontinuities.

1-4 Thesis outline

The rest of the MSc thesis is organized as follows.

Chapter 2 introduces a new dynamic quantizer with adjustable offset to handle the tracking case. A hybrid adaptive control policy is derived to achieve asymptotic tracking in the quantized input model reference adaptive control scheme.

Chapter 3 generalizes the hybrid adaptive control policy obtained in Chapter 2, for the case of quantized input uncertain switched linear systems, driven by a switching time policy. A time-varying Lyapunov function is used to design the adaptive law so that asymptotic tracking can be achieved without zooming out at every switching instant.

Chapter 4 verifies the effectiveness of the proposed methodology via simulations: the adaptive hybrid control policy described in Chapter 2 is applied to the case study of an electro-hydraulic system. The adaptive law using a time-scheduled Lyapunov function introduced in Chapter 3, is evaluated via a case study of NASA GTM model linearized at multiple points.

Finally, **Chapter 5** concludes this MSc thesis and gives some recommendations for future work.

Chapter 2

Quantized adaptive tracking for uncertain linear systems

This chapter is organized as follows: Section 2-1 formulates the quantized control problem. The adaptive control design is established in Section 2-2, while Section 2-3 presents the main stability and tracking results.

2-1 Problem statement

Let us consider the linear time-invariant system

$$\dot{x}(t) = Ax(t) + Bg_{\eta\mu}(u(t)) \tag{2-1}$$

where $x \in \mathbb{R}^n$ is the state, $u \in \mathbb{R}^q$ is the control input, $g_{\eta\mu}(u) : \mathbb{R}^q \to Q$, where $Q \subset \mathbb{R}^q$, is the input quantizer (to be defined later), and the matrices $A \in \mathbb{R}^{n\times n}$ and $B \in \mathbb{R}^{n\times q}$ are *unknown* constant matrices.

2-1-1 Linear reference model system and controller structure

We consider the following linear reference model:

$$\dot{x}_{\mathrm{m}} = A_{\mathrm{m}}x_{\mathrm{m}}(t) + B_{\mathrm{m}}r(t) \tag{2-2}$$

where $A_{\mathrm{m}} \in \mathbb{R}^{n\times n}$, $B_{\mathrm{m}} \in \mathbb{R}^{n\times q}$ are constant *known* matrices with A_{m} a Hurwitz matrix, $r \in \mathbb{R}^q$ is a bounded continuous reference input signal and $x_{\mathrm{m}} \in \mathbb{R}^n$ is the desired state to track.

The following assumptions are made in order to have a well-posed adaptive problem:

Assumption 1. *There exist a constant matrix $K_{\mathrm{x}}^* \in \mathbb{R}^{n\times q}$ and an invertible constant matrix $K_{\mathrm{r}}^* \in \mathbb{R}^{q\times q}$ such that*

$$A_{\mathrm{m}} = A + BK_{\mathrm{x}}^{*T},\ B_{\mathrm{m}} = BK_{\mathrm{r}}^*. \tag{2-3}$$

Assumption 2. *There exists a known matrix $S \in \mathbb{R}^{q\times q}$ such that*

$$\Gamma = K_{\mathrm{r}}^* S \tag{2-4}$$

is positive definite.

Assumption 3. *A and B in (2-1) belong to a known and bounded uncertainty set Θ.*

Remark 1. *Assumption 1 is required for the existence of a closed-loop that matches (2-1) to the reference model (2-2) (well-posedness). Assumption 2 generalizes the classical condition of knowing the sign of the input vector field in the multivariable case. Both assumptions are, up to now, the most relaxed conditions for ensuring closed-loop signal boundedness in multivariable adaptive control [4], [42], and will be adopted also in our input quantization setting. Assumption 3 is required to obtain a bound to the increasing rate of the tracking error during the zooming-in phase, as it will be explained in Section 2-3.*

Being A and B in (2-1) unknown, the control gains K_{x}^* and K_{r}^* in (2-3) cannot be implemented and must be estimated. Inspired by [4], the following adaptive state-feedback controller is applied:

$$u(t) = K_{\mathrm{x}}^T(t)x(t) + K_{\mathrm{r}}(t)r(t). \tag{2-5}$$

We consider a networked control setup with the controller on the sensor side, so that the control input (2-5) must be quantized and sent to the actuator via a communication channel. The next section introduces a quantizer appropriate to our control goals.

2-1-2 Dynamic quantizer design

It must be noted though, that the quantizers commonly adopted in the literature [14], [16], are anti-symmetric with respect to zero: as such, they can increase precision only around zero, and thus they are appropriate only for regulation problems. If we adopted standard uniform quantizers for the tracking case we would get

$$g(u) = g(K_{\mathrm{x}}^T x + K_{\mathrm{r}} r) = g\Big(K_{\mathrm{x}}^T(x - x_{\mathrm{m}}) + K_{\mathrm{x}}^T x_{\mathrm{m}} + K_{\mathrm{r}} r\Big) \tag{2-6}$$

from which we notice that, if we define the state-tracking error

$$e = x - x_{\mathrm{m}} \tag{2-7}$$

then, for $e \to 0$ the quantized input converges to $g(K_{\mathrm{x}}^T x_{\mathrm{m}} + K_{\mathrm{r}} r)$ and asymptotic tracking would be in general impossible due to finite precision of the quantizer around $K_{\mathrm{x}}^T x_{\mathrm{m}} + K_{\mathrm{r}} r$.

With this problem in mind, we introduce an adjustable offset $\eta(t)$ in the quantizer, so as to achieve quntization anti-symmetry around $\eta(t) = K_{\mathrm{x}}^T(t)x_{\mathrm{m}}(t) + K_{\mathrm{r}}(t)r(t)$. We define the following dynamic quantizer:

$$g_{\eta\mu}(u) = \mu g\left(\frac{u-\eta}{\mu}\right) \tag{2-8}$$

where the time index t has been (and will be when appropriate) omitted for compactness. Note that the dynamic quantizer in (2-8) satisfies, analogously to (1-1), the following condition:

$$\mu\left\|g\left(\frac{u-\eta}{\mu}\right)\right\| \leq \mu M \tag{2-9}$$

where μM represents the quantization range of the dynamic quantizer. In case of no saturation, the quantizer must satisfy analogously to (1-2), the additional requirement:

$$\left\|\mu g\left(\frac{u-\eta}{\mu}\right) - u\right\| = \mu\left\|g\left(\frac{u-\eta}{\mu}\right) - \frac{u}{\mu}\right\| \leq \mu\Delta \tag{2-10}$$

where $\mu\Delta$ represents the quantization error in the dynamic quantizer, when no saturation occurs. The situation with the proposed quantizer (2-8) is depicted in Fig. 2-1.

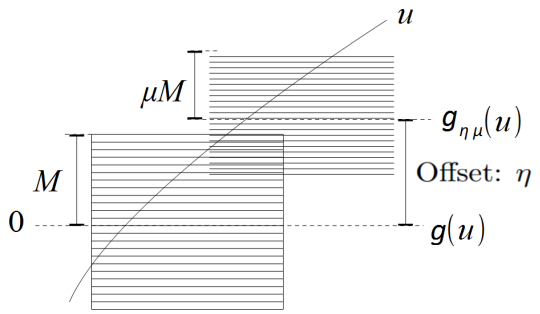

Figure 2-1: Dynamic quantizer with adjustable offset

Remark 2. *As the zooming mechanism of state-of-the-art quantizer is typically explained in terms of digital videos, we can also give an explanation to the proposed quantizer in similar terms. In fact, dynamic offsets are often used in video encoding: in many H.264-based compression protocols the encoder is regulated on a frame level (offset) to obtain the number of bits that is very close to the allocated one [43], [44]. The frame level is also encoded and can be adjusted. Several mechanisms have been defined to tune the offset of the quantizer based on the previous frames [45], [46], so as to improve the compression ratio (increase the video resolution given the allocated bit rate, or reduce the bit rate given a desired video resolution). As these video encoding mechanisms are able to increase the resolution around similar frames close in time, similarly our proposed quantizer increases the resolution around a changing offset in order to achieve asymptotic tracking.*

2-1-3 Problem formulation

We are now ready to formulate our control objective:

Problem 1. ***Input-quantized model reference adaptive control****: Design an adaptive control law for the control gains in (2-3), and adjustment strategies for the dynamic range μ and dynamic offset η in (2-8) such that, without requiring the knowledge of A and B in (2-1), the state trajectories of the system (2-1) track asymptotically the trajectories generated by the reference model (2-2).*

A schematic representation of the proposed adaptive NCS is shown in Fig. 2-2.

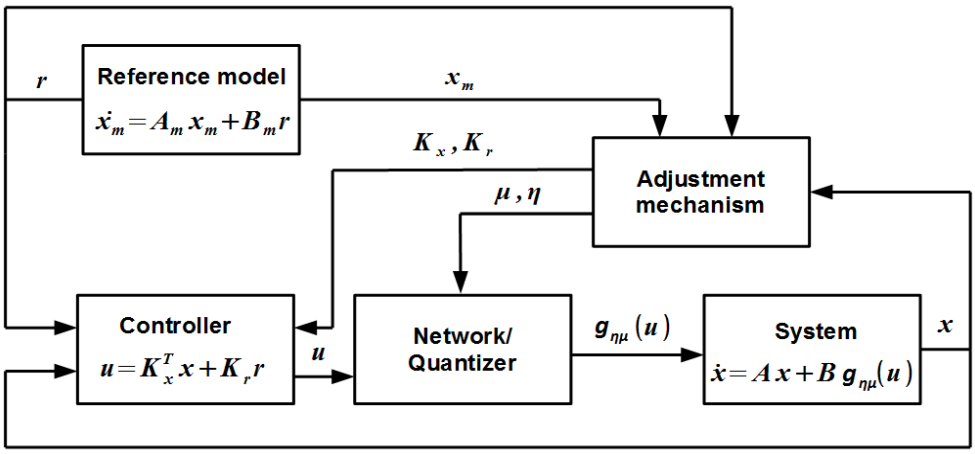

Figure 2-2: Adaptive NCS in the MRAC framework

2-2 Adaptive law controller design

Since A_{m} in (2-2) must be Hurwitz, so as to generate a bounded signal state x_{m} from bounded r, there exist positive definite matrices $P \in \mathbb{R}^{n\times n}$, $Q \in \mathbb{R}^{n\times n}$, such that the following inequality holds:

$$A_{\mathrm{m}}^T P + P A_{\mathrm{m}} \leq -Q. \tag{2-11}$$

When the quantized adaptive state-feedback controller given by (2-5), (2-8), is applied to (2-1), the closed-loop system reads as:

$$\dot{x} = Ax + B(K_{\mathrm{x}}^T x + K_{\mathrm{r}} r) + \mu B \underbrace{\left[g\left(\frac{K_{\mathrm{x}}^T x + K_{\mathrm{r}} r - \eta}{\mu} \right) - \frac{K_{\mathrm{x}}^T x + K_{\mathrm{r}} r}{\mu} \right]}_{\Delta_{\mathrm{u}}} \tag{2-12}$$

where in case of no saturation, it holds from (1-2), $\|\Delta_{\mathrm{u}}\| \leq \Delta$.

In view of (2-2) and (2-12), the evolution of the tracking error can be written as:

$$\dot{e} = \dot{x} - \dot{x}_{\mathrm{m}} = A_{\mathrm{m}}e + B\tilde{K}_{\mathrm{x}}^{T}x + B\tilde{K}_{\mathrm{r}}r + B\mu\Delta_{\mathrm{u}} \tag{2-13}$$

where $\tilde{K}_{\mathrm{x}} = K_{\mathrm{x}} - K_{\mathrm{x}}^{*}$, $\tilde{K}_{\mathrm{r}} = K_{\mathrm{r}} - K_{\mathrm{r}}^{*}$, are defined as the controller parameter errors.

In order to analyze the stability of the closed-loop system (2-13), the following Lyapunov-like function is considered:

$$V = e^{T}Pe + tr\Big[\tilde{K}_{\mathrm{x}}\Gamma^{-1}\tilde{K}_{\mathrm{x}}^{T}\Big] + tr\Big[\tilde{K}_{\mathrm{r}}^{T}\Gamma^{-1}\tilde{K}_{\mathrm{r}}\Big] \tag{2-14}$$

with $\Gamma \in \mathbb{R}^{q\times q}$ coming from (2-4).

The time derivative of (2-14) is

$$\begin{aligned}\dot{V} &= \dot{e}^{T}Pe + e^{T}P\dot{e} + 2tr\Big[\tilde{K}_{\mathrm{x}}\Gamma^{-1}\dot{\tilde{K}}_{\mathrm{x}}\Big] + 2tr\Big[\tilde{K}_{\mathrm{r}}\Gamma^{-1}\dot{\tilde{K}}_{\mathrm{r}}\Big] \\ &= e^{T}[A_{m}^{T}P + PA_{m}]e + 2x^{T}\tilde{K}_{\mathrm{x}}B^{T}Pe + 2r^{T}\tilde{K}_{\mathrm{r}}^{T}BPe + 2tr\Big[\tilde{K}_{\mathrm{x}}\Gamma^{-1}\dot{\tilde{K}}_{\mathrm{x}}\Big] + 2tr\Big[\tilde{K}_{\mathrm{r}}\Gamma^{-1}\dot{\tilde{K}}_{\mathrm{r}}\Big] \\ &\quad + 2e^{T}PB\mu\Delta_{\mathrm{u}}\end{aligned} \tag{2-15}$$

Looking at (2-15), we propose the controller parameter adaptation law as follows:

$$\begin{aligned}2x^{T}\tilde{K}_{\mathrm{x}}B^{T}Pe &= 2tr\Big[x^{T}\tilde{K}_{\mathrm{x}}B^{T}Pe\Big] = 2tr\Big[\tilde{K}_{\mathrm{x}}B^{T}Pex^{T}\Big] = -2tr\Big[\tilde{K}_{\mathrm{x}}\Gamma^{-1}\dot{\tilde{K}}_{\mathrm{x}}^{T}\Big] \\ 2r^{T}\tilde{K}_{\mathrm{r}}^{T}B^{T}Pe &= 2tr\Big[r^{T}\tilde{K}_{\mathrm{r}}^{T}B^{T}Pe\Big] = 2tr\Big[\tilde{K}_{\mathrm{r}}^{T}B^{T}Per^{T}\Big] = -2tr\Big[\tilde{K}_{\mathrm{r}}^{T}\Gamma^{-1}\dot{\tilde{K}}_{\mathrm{r}}\Big]\end{aligned} \tag{2-16}$$

In view of Assumption 3, lower and upper bounds for the controller parameters K_{x}, K_{r} can be found (this can be done by testing the matching conditions (2-3) over the uncertainty set Θ). More precisely, let the upper (lower) bounds be represented by $\overline{K}_{\mathrm{x}}$, ($\underline{K}_{\mathrm{x}}$), $\overline{K}_{\mathrm{r}}$, ($\underline{K}_{\mathrm{r}}$) for the controller parameter estimates K_{x}, K_{r} respectively. If we define

$$\begin{aligned}K_{\mathrm{x}}^{T} &= \begin{bmatrix}k_{\mathrm{x1}} & k_{\mathrm{x2}} & \cdots & k_{\mathrm{xi}}\end{bmatrix},\ i = 1,2,...,n \\ K_{\mathrm{r}} &= \begin{bmatrix}k_{\mathrm{r1}} & k_{\mathrm{r2}} & \cdots & k_{\mathrm{rj}}\end{bmatrix},\ j = 1,2,...,q\end{aligned} \tag{2-17}$$

and assume $k_{\mathrm{xi}}^{*} \in [\underline{k}_{\mathrm{xi}}, \overline{k}_{\mathrm{xi}}]$, $k_{\mathrm{rj}}^{*} \in [\underline{k}_{\mathrm{rj}}, \overline{k}_{\mathrm{rj}}]$, then for $t \geq 0$ we require

$$\begin{aligned}k_{\mathrm{xi}}(t) &\in [\underline{k}_{\mathrm{xi}}, \overline{k}_{\mathrm{xi}}],\ i = 1,2,...,n \\ k_{\mathrm{rj}}(t) &\in [\underline{k}_{\mathrm{rj}}, \overline{k}_{\mathrm{rj}}],\ j = 1,2,...,q\end{aligned} \tag{2-18}$$

Using (2-4), (2-16) results in the following parameter projection adaptive law:

$$\begin{aligned}\dot{K}_{\mathrm{x}}^{T} &= -S^{T}B_{\mathrm{m}}^{T}Pex^{T} + F_{\mathrm{x}}^{T} \\ \dot{K}_{\mathrm{r}} &= -S^{T}B_{\mathrm{m}}^{T}Per^{T} + F_{\mathrm{r}}\end{aligned} \tag{2-19}$$

where $F_{\mathrm{x}}^T = \begin{bmatrix} f_{\mathrm{x1}} & f_{\mathrm{x2}} & \cdots & f_{\mathrm{xi}} \end{bmatrix}$, $i = 1, 2, ..., n$, and $F_{\mathrm{r}} = \begin{bmatrix} f_{\mathrm{r1}} & f_{\mathrm{r2}} & \cdots & f_{\mathrm{rj}} \end{bmatrix}$, $j = 1, 2, ..., q$, are the projection terms to confine the controller parameters within their known bounds.

More precisely, for $t \geq 0$:

$$\text{If } k_{\mathrm{xi}}(t) \in (\underline{k}_{\mathrm{xi}}, \overline{k}_{\mathrm{xi}}) \implies f_{\mathrm{xi}}(t), = 0 \tag{2-20a}$$
$$\text{If } k_{\mathrm{xi}}(t) = \underline{k}_{\mathrm{xi}}, (\overline{k}_{\mathrm{xi}}) \ \&\ \dot{k}_{\mathrm{xi}}(t), (\dot{k}_{\mathrm{xi}}(t)) = 0 \implies f_{\mathrm{xi}}(t) = 0 \tag{2-20b}$$
$$\text{If } k_{\mathrm{rj}}(t) \in (\underline{k}_{\mathrm{rj}}, \overline{k}_{\mathrm{rj}}) \implies f_{\mathrm{rj}}(t) = 0 \tag{2-20c}$$
$$\text{If } k_{\mathrm{rj}}(t) = \underline{k}_{\mathrm{rj}}, (\overline{k}_{\mathrm{rj}}) \ \&\ \dot{k}_{\mathrm{rj}}(t), (\dot{k}_{\mathrm{rj}}(t)) = 0 \implies f_{\mathrm{rj}}(t) = 0 \tag{2-20d}$$
$$\text{If } k_{\mathrm{xi}}(t) = \underline{k}_{\mathrm{xi}},\ (\overline{k}_{\mathrm{xi}}) \ \&\ \dot{k}_{\mathrm{xi}}(t) < 0,\ (\dot{k}_{\mathrm{xi}}(t) > 0) \implies f_{\mathrm{xi}}(t) = -h_{\mathrm{xi}}(t) \tag{2-20e}$$
$$\text{If } k_{\mathrm{rj}}(t) = \underline{k}_{\mathrm{rj}},\ (\overline{k}_{\mathrm{rj}}) \ \&\ \dot{k}_{\mathrm{rj}}(t) < 0,\ (\dot{k}_{\mathrm{rj}}(t) > 0) \implies f_{\mathrm{rj}}(t) = -h_{\mathrm{rj}}(t) \tag{2-20f}$$

where

$$\begin{aligned} H_{\mathrm{x}}^T &= \begin{bmatrix} h_{\mathrm{x1}} & h_{\mathrm{x2}} & \cdots & h_{\mathrm{xn}} \end{bmatrix} = -S^T B_{\mathrm{m}}^T P e x^T \\ H_{\mathrm{r}} &= \begin{bmatrix} h_{\mathrm{r1}} & h_{\mathrm{r2}} & \cdots & h_{\mathrm{rq}} \end{bmatrix} = -S^T B_{\mathrm{m}}^T P e r^T. \end{aligned} \tag{2-21}$$

Using (2-19) and the properties of F_{x} and F_{r} in (2-20), the time derivative of (2-15) along (2-13) is:

$$\dot{V} = e^T (A_{\mathrm{m}} P + P A_{\mathrm{m}}) e + \underbrace{2tr\left[\tilde{K}_{\mathrm{x}} \Gamma^{-1} F_{\mathrm{x}}^T\right] + 2tr\left[\tilde{K}_{\mathrm{r}}^T \Gamma^{-1} F_{\mathrm{r}}\right]}_{K_{\mathrm{v}}} + 2e^T P B \mu \Delta_{\mathrm{u}}. \tag{2-22}$$

Lemma 2-2.1. *[36] Assume $K_{\mathrm{x}}, K_{\mathrm{r}} \in \mathbb{R}$ and let t_0 be a time instant such that $t_0 \geq 0$. Then, it is true that*

$$\tilde{K}_{\mathrm{x}}(t_0) F_{\mathrm{x}}(t_0),\ \tilde{K}_{\mathrm{r}}(t_0) F_{\mathrm{r}}(t_0) \leq 0 \tag{2-23}$$

Proof. One can distinguish two cases with accordance to (2-20):

Case (a): Let $K_{\mathrm{x}}(t_0) = \overline{K}_{\mathrm{x}},\ (\underline{K}_{\mathrm{x}})$. If additionally, $\dot{K}_{\mathrm{x}}(t_0) > 0$, $(\dot{K}_{\mathrm{x}}(t_0) < 0)$, we have from (2-20e): $F_{\mathrm{x}}(t_0) < 0$, $(F_{\mathrm{x}}(t_0) > 0)$.
Thus, $\tilde{K}_{\mathrm{x}}(t_0) = \overline{K}_{\mathrm{x}} - K_{\mathrm{x}}^* > 0$, $(\underline{K}_{\mathrm{x}} - K_{\mathrm{x}}^* < 0\ ) \implies$

$$\tilde{K}_{\mathrm{x}}(t_0) F_{\mathrm{x}}(t_0),\ (\tilde{K}_{\mathrm{x}}(t_0) F_{\mathrm{x}}(t_0)) < 0. \tag{2-24}$$

Case (b): Let $K_{\mathrm{x}}(t_0) \in (\underline{K}_{\mathrm{x}}, \overline{K}_{\mathrm{x}})$. Because of (2-20a), it holds:

$$\tilde{K}_{\mathrm{x}}(t_0) F_{\mathrm{x}}(t_0) = 0. \tag{2-25}$$

A schematic representation of the two cases, (a), (b), can be shown in Fig. 2-3.

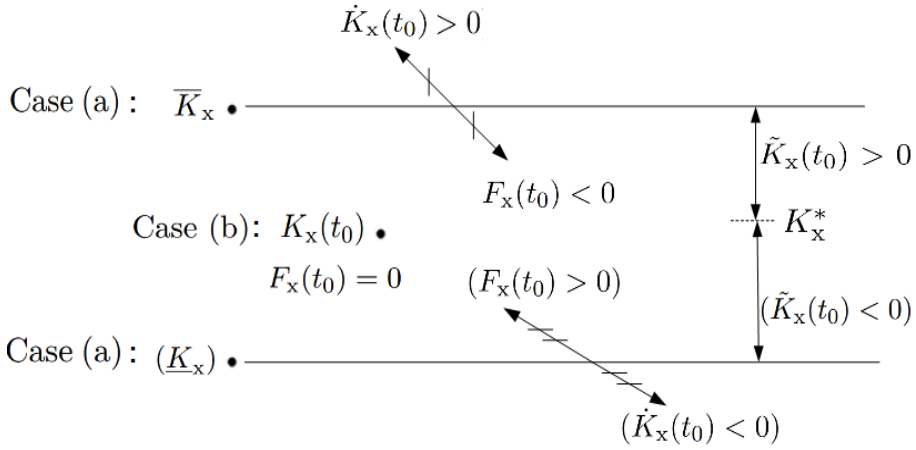

Figure 2-3: Parameter adaptive projection law

Then, (2-24), (2-25), imply $\tilde{K}_x(t_0)F_x(t_0) \leq 0$. With similar argumentation we can conclude that $\tilde{K}_r(t_0)F_r(t_0) \leq 0$. This completes the proof. □

Lemma 2-2.1 can be easily extended to the multivariable case, thus it holds for K_v in (2-22)

$$K_v \leq 0. \tag{2-26}$$

Using (2-11) and (2-26), (2-22) results in

$$\dot{V} \leq -e^T Qe + 2e^T PB\mu\Delta_u. \tag{2-27}$$

Because, K_x, K_r are bounded due to the projection terms in (2-19), we can define $\rho \in \mathbb{R} \geq 0$ such that:

$$\rho = \max_{t \geq 0} \left\{ tr\left[\tilde{K}_x \Gamma^{-1} \tilde{K}_x^T\right] + tr\left[\tilde{K}_r^T \Gamma^{-1} \tilde{K}_r\right] \right\} \tag{2-28}$$

and because of (2-14), we have

$$e^T Pe \leq V \leq e^T Pe + \rho. \tag{2-29}$$

Because P is positive definite, the following inequality from linear algebra is known:

$$\lambda_{min}(P)\|e\|^2 \leq e^T Pe \leq \lambda_{max}(P)\|e\|^2 \tag{2-30}$$

with $\lambda_{max}(P) \geq \lambda_{min}(P) > 0$.

2-3 Hybrid control policy

Inspired by [14], the time derivative of V in (2-27), in case of no saturation, it can be equivalently expressed as

$$\begin{aligned}\dot{V} &\leq -e^T Q e + 2e^T P B \mu \Delta_{\mathrm{u}} \leq -\lambda_{min}(Q)\|e\|^2 + 2e^T P B \mu \Delta \\ &\leq -\lambda_{min}(Q)\|e\| \left(\|e\| - \underbrace{\frac{2\max_{B\in\Theta}\|PB\|}{\lambda_{min}(Q)}}_{R} \mu\Delta \right) \implies\end{aligned}$$

$$\dot{V} \leq -\|e\|\,\lambda_{min}(Q)(\|e\| - \mu R\Delta) \tag{2-31}$$

where R is bounded. According to (2-9), the requirement of no saturation can be equivalently expressed by the following condition:

$$\|u - \eta\| \leq \mu M. \tag{2-32}$$

Because the controller parameter estimates K_{x}, K_{r} are bounded in view of Assumption 3, we define

$$\overline{K}_{\mathrm{x}} = \max_{t\geq 0} \|K_{\mathrm{x}}\|\,. \tag{2-33}$$

Considering $\|u - \eta\| = \left\| K_{\mathrm{x}}^T x + K_{\mathrm{r}} r - K_{\mathrm{x}}^T x_{\mathrm{m}} - K_{\mathrm{r}} r \right\| = \left\| K_{\mathrm{x}}^T (x - x_{\mathrm{m}} \right\|$, the condition of saturation given by (2-32) is satisfied if the following condition holds:

$$\|e\| \leq \frac{\mu M}{\overline{K}_{\mathrm{x}}}. \tag{2-34}$$

We define the following regions:

$$\mathscr{B}_1(\mu) := \left\{ e : \|e\| \leq \frac{\mu M}{\overline{K}_{\mathrm{x}}} \right\} \tag{2-35a}$$

$$\mathscr{I}_1(\mu) := \left\{ e : e^T P e \leq \lambda_{min}(P) \frac{\mu^2 M^2}{\overline{K}_{\mathrm{x}}^2} \right\} \tag{2-35b}$$

$$\mathscr{B}_2(\mu) := \left\{ e : \|e\| \leq \mu R \Delta \right\} \tag{2-35c}$$

$$\mathscr{I}_2(\mu) := \left\{ e : e^T P e \leq \lambda_{max}(P) \mu^2 R^2 \Delta^2 \right\}. \tag{2-35d}$$

Note that, when

$$\frac{\sqrt{\lambda_{min}(P)} M}{\overline{K}_{\mathrm{x}}} > \sqrt{\lambda_{max}(P)} R \Delta$$

then $\mathscr{B}_2(\mu) \subset \mathscr{I}_2(\mu) \subset \mathscr{I}_1(\mu) \subset \mathscr{B}_1(\mu)$. The situation is depicted graphically in Fig. 2-4.

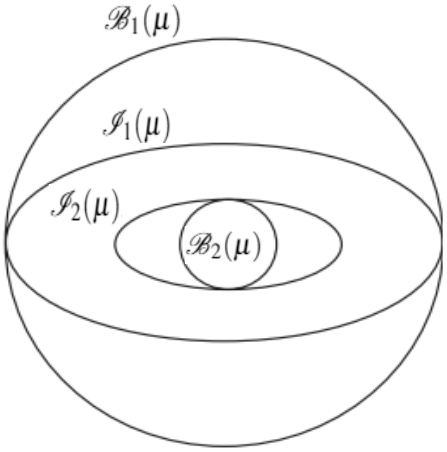

Figure 2-4: Regions of interest

2-3-1 Main result

Using the previously explained design, the following stability result can be derived:

Theorem 2-3.1. *Consider the input-quantized model reference adaptive control given by system (2-1), reference model (2-2), quantizer (2-8), adaptive laws (2-19). If the following holds*

$$\frac{\sqrt{\lambda_{min}(P)}M}{\overline{K}_{\mathrm{x}}} > \sqrt{\lambda_{max}(P)}R\Delta \tag{2-36}$$

then there exists an error-based hybrid quantized feedback control policy that makes the closed-loop system (2-13) globally asymptotically stable with $\lim_{t\to\infty} e(t) = 0$.

Proof. The hybrid quantized feedback control policy is designed in a constructive way along the proof. Following a similar approach as in [14] we distinguish two phases, namely the zooming-in and zooming-out phases. In the zooming-out phase, μ is chosen so that $e \in \mathscr{B}_1(\mu)$ and thus boundedness can be guaranteed. During zooming-in phase, the objective is to shrink the smaller region $\mathscr{I}_2(\mu)$ by reducing the dynamic quantizer parameter μ so that state-tracking properties can be concluded. The two phases are examined thoroughly as follows:

Zooming-out phase: Let $\mu(0) = 1$. If $\|e(0)\| > \frac{M}{\overline{K}_{\mathrm{x}}}$, in view of (2-34), saturation is detected in the quantizer. In this case, we make $\mu(t)$ increase in a piecewise fashion fast enough to dominate the growth factor of e which can be seen by (2-13) that equals $\left|e^{\max_{A,B\in\Theta}\|A+BK_{\mathrm{x}}^T\|}\right|$, where $\max_{A,B\in\Theta}\left\|A+BK_{\mathrm{x}}^T\right\|$ is bounded in view of Assumption 3. There will be a time instant $t_0 \geq 0$ and a bounded $\mu(t_0)$ at which the following relation will be true

$$\|e(t_0)\| \leq \sqrt{\frac{\lambda_{min}(P)}{\lambda_{max}(P)}}\frac{\mu(t_0)M}{\overline{K}_{\mathrm{x}}} \tag{2-37}$$

and as a consequence of (2-30), (2-35a), and (2-35b), it holds $e(t_0) \in \mathscr{I}_1(\mu(t_0)) \cap \mathscr{B}_1(\mu(t_0))$. Because $e(t_0) \in \mathscr{B}_1(\mu(t_0))$ and $\mathscr{B}_2(\mu) \subset \mathscr{B}_1(\mu)$ from (2-36), we get from (2-31) $\dot{V} \leq 0$. Thus, for $t \geq t_0$ when $e(t) \in \mathscr{B}_1(\mu(t_0))$ and $e(t) \notin \mathscr{B}_2(\mu(t_0))$ we have

$$\dot{V} \leq 0 \implies V(t) \leq V(t_0) \implies \|e(t)\| \leq \sqrt{\frac{\mu^2(t_0)M^2}{\overline{K}_{\mathrm{x}}{}^2} + \frac{\rho}{\lambda_{min}(P)}} \tag{2-38}$$

which implies, with accordance to (2-35a), that $e(t)$ does not necessarily belong to $B_1(\mu(t_0))$. Then, for $t \geq t_0$ we might have two cases: either the norm of the tracking error is decreasing, in which case there is no saturation and we go to the zooming-in phase; or the norm of the tracking error is increasing in which case we keep increasing $\mu(t)$ at the same rate. For this second case, because $\mu(t)$ is updated continuously at much higher rate compared to the growth of $e(t)$ to avoid saturation, we can assume that $\forall t \geq t_0$, $e(t) \in \mathscr{B}_1(\mu(t))$. If additionally $e \notin \mathscr{B}_2(\mu)$, implying $\dot{V} \leq 0$ for $t \geq t_0$, the following inequality is true:

$$\|e(t)\| \leq \sqrt{\frac{V(t_0)}{\lambda_{\min}(P)}} \implies e(t) \in \mathscr{L}_\infty. \tag{2-39}$$

Zooming-in phase: Let t' be a time instant such that $t \geq t' \geq t_0$, and $e(t) \in \mathscr{B}_1(\mu(t'))$. Then it is true that $\dot{V} \leq 0$ as long as $e \notin \mathscr{B}_2(\mu(t'))$. One can see from (2-35) and Fig. 2-4, that $\mathscr{B}_2(\mu) \subset \mathscr{I}_2(\mu)$. Thus, at time $\tilde{t}$ with $\tilde{t} \geq t'$, when $e(t) \in \mathscr{I}_2(\mu(t'))$, $\mu(\tilde{t})$ is updated

$$\mu(\tilde{t}) = \underbrace{\frac{\overline{K}_{\mathrm{x}}\sqrt{\lambda_{\max}(P)}R\Delta}{\sqrt{\lambda_{\min}(P)}M}}_{\Omega}\mu(t'). \tag{2-40}$$

Obviously $\Omega < 1$ due to (2-36). Thus, zooming-in event occurs, and one can see that $\mathscr{I}_1(\mu(\tilde{t})) = \mathscr{I}_2(\mu(t'))$, where $\mu(t')$ is the value of μ that prevents saturation (according to (2-37)), with $\mu(t_0)$ replaced by $\mu(t')$. After the zooming-in event one might have two cases: either the tracking error increases tending to violate $e \in \mathscr{B}_1(\mu(\tilde{t}))$, in which case a new zooming-out phase is activated; or the tracking error keeps decreasing in which case a new zooming-in will eventually be triggered. In the second case, since μ is updated when $e \in \mathscr{I}_2(\mu)$ and because $\mathscr{B}_2(\mu) \subset \mathscr{I}_2(\mu)$, it is true that $\dot{V} \leq 0$ and as a consequence (2-38) holds, implying $e(t) \in \mathscr{L}_\infty$. Additionally, because of (2-7) and because x_{m} is bounded, it is true that $x \in \mathscr{L}_\infty$. By looking at (2-13) and (2-22) we can see by using similar argumentation that $\dot{e}$ and $\dot{V}$ consist of bounded terms, and thus they are bounded. The following lemma will be useful in our stability analysis.

Lemma 2-3.2. *[47]* ***(Generalized Barbalat's lemma)*** *Suppose* $V(t) : [0, \infty) \to \mathbb{R}$ *satisfies*

1. $\lim_{t\to\infty} V(t)$ *exists (*$V(t)$ *is lower bounded);*
2. $\dot{V(t)}$ *is negative semi-definite* ($\dot{V(t)} \leq 0$)*;*
3. $\ddot{V(t)}$ *is finite (well-defined) when* $\dot{V(t)}$ *switches,*

then it is true $\lim_{t\to\infty} \dot{V(t)} = 0$.

Let us now look at the combined behavior of zooming-in and zooming-out phases. For $t \geq t_0$, at both zooming-in and zooming-out phases it holds $\dot{V} \leq 0 \implies V(t) \leq V(t_0)$, thus V is lower-bounded by $V(t_0)$. Because $\ddot{V}$ is bounded and V is lower bounded by $V(t_0)$, because it holds $\dot{V} \leq 0 \; \forall t \geq t_0$, we can conclude using generalized Barbalat's lemma, $\lim_{t\to\infty} \dot{V}(t) = 0$.

The following relation from (2-31) holds:

$$\begin{aligned} \lim_{t\to\infty} \dot{V}(t) \leq -\lim_{t\to\infty} \|e(t)\| \, \lambda_{\min}(Q) \Big(\|e(t)\| - \mu(t) R\Delta \Big) \implies \\ 0 \leq -\lim_{t\to\infty} \|e(t)\| \, \lambda_{\min}(Q) \Big(\|e(t)\| - \mu(t) R\Delta \Big). \end{aligned} \tag{2-41}$$

The above relation is true when

$$\lim_{t\to\infty} \|e(t)\| = 0 \quad \text{or} \quad \lim_{t\to\infty} \|e(t)\| - \mu(t) R\Delta \leq 0. \tag{2-42}$$

The second relation implies that $e \in \mathscr{B}_2(\mu)$. However when $e \in \mathscr{I}_2(\mu)$, and because $\mathscr{I}_2(\mu) \supset \mathscr{B}_2(\mu)$, μ is decreasing as in (2-40) because zooming-in occurs, and consequently $e \notin \mathscr{B}_2(\mu)$. As a consequence $\lim_{t\to\infty} \mu(t) = 0$ and by (2-42) we conclude $\lim_{t\to\infty} \|e(t)\| = 0$. Because all signals are bounded and $\lim_{t\to\infty} e(t) = 0$, we can conclude (2-13) is globally asymptotically stable. □

A state flow diagram of the adaptive hybrid control strategy is shown in Fig. 2-5.

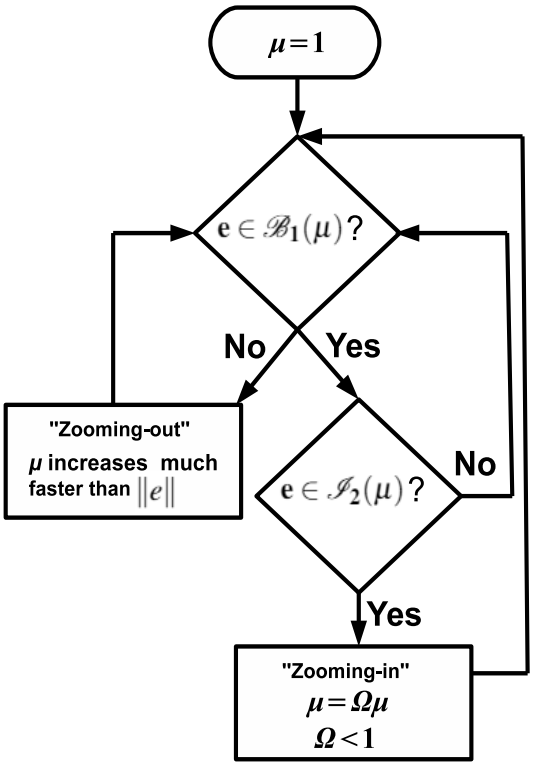

Figure 2-5: Error dependent adaptive hybrid control strategy

Remark 3. *In [14] a hybrid time-dependent switching strategy is used for updating the values of μ. More precisely an upper bound T is derived on the time interval T such that if $e(t_0) \in \mathscr{I}_1(\mu(t_0)) \implies e(t_0+T) \in \mathscr{I}_2(\mu(t_0))$ and then μ is updated as $\mu(t_0+T) = \Omega\mu(t_0)$. This is not applicable to the adaptive control case, unless additional requirements on $\|e\|$ are imposed, because V in (2-14) is given in terms of inequalities. The error-dependent switching strategy we employ in this work relies on on-line evaluation of the tracking error to determine the time instants at which e enters a certain region. This can give more reliability and robustness with respect to modelling errors.*

Remark 4. *It has to be underlined that the term "zooming-in phase" was originally adopted in literature [14] with reference to the fact that that μ decreases monotonically. Later, the same term has been adopted also in settings where the decrease of μ was not monotonic (e.g. in switched systems [48]). The proof of Theorem 2-3.1 shows that also in our adaptive setting the decrease of μ may be not monotonic. In our case, we recover the original meaning by using the term "zooming-in phase" only when smaller regions $\mathscr{I}_1(\mu)$, $\mathscr{I}_2(\mu)$ are obtained. For this reason we might have multiple zooming-in and zooming-out phases, as it will be illustrated in Section 4-1.*

2-4 Summary

The adaptive asymptotic state-tracking control problem in the model reference adaptive control case, with quantized input measurements has been investigated. A hybrid control policy has been applied to a novel dynamic quantizer with adjustable offset, and it was proven to guarantee global asymptotic stability and state-tracking. A practical example of an electro-hydraulic system will be used in Section 4-1 to demonstrate the effectiveness of the proposed hybrid control scheme.

Chapter 3

Quantized adaptive tracking for uncertain switched linear systems

This Chapter is organized as follows: Section 3-1 introduces the quantized control problem. The adaptive control design is established in Section 3-2 and Section 3-3 presents the stability and tracking results. The interested reader must check Appendix A for preliminaries for the stability of switched linear systems driven by a time-scheduled policy, which are the background for the results in this Chapter.

3-1 Problem statement

Let us consider the uncertain time-driven switched linear system

$$\dot{x}(t) = A_{\sigma(t)}x(t) + B_{\sigma(t)}g_{\eta\mu}(u(t)),\ \sigma(t) \in \mathscr{N} = \{1, ..., N\} \tag{3-1}$$

where $x \in \mathbb{R}^n$ is the state, $u \in \mathbb{R}^q$ is the control input, $g_{\eta\mu}(u) : \mathbb{R}^q \to Q$, with $Q \subset \mathbb{R}^q$, is the input quantizer given by (2-8), and $\sigma(\cdot)$ is a piecewise switching law taking values in $\mathscr{N}$, where N denotes the number of subsystems. The system is uncertain because the matrices $A_p \in \mathbb{R}^{n\times n}$, $B_p \in \mathbb{R}^{n\times q}$ are *unknown* constant matrices for all $p \in \mathscr{N}$. The switching law $\sigma(\cdot)$ satisfies the following slowly-switching constraint:

Definition 3-1.1. *[34] (**Dwell-time switching**) A switching law defining a switching sequence $S := \{t_1, t_2, ...\}$ is admissible with dwell-time if there exists a number $\tau_d \geq 0$ such that $t_{i+1} - t_i \geq \tau_d$, $\forall i \in \mathbb{N}^+$. Any τ_d that satisfies these constraints is called dwell-time and the set of admissible with dwell-time switching laws is denoted by $\mathscr{D}(\tau_d)$.*

3-1-1 Switched linear reference model system and controller structure

Let us consider the following switched linear reference model:

$$\dot{x}_{\mathrm{m}}(t) = A_{\mathrm{m}\sigma(t)}x_{\mathrm{m}}(t) + B_{\mathrm{m}\sigma(t)}r(t),\ \sigma(t) \in \mathscr{N} \tag{3-2}$$

where $x_{\mathrm{m}} \in \mathbb{R}^n$ is the desired state vector to track and $r \in \mathbb{R}^q$ is a bounded continuous reference input signal. The matrices $A_{\mathrm{m}p} \in \mathbb{R}^{n\times n}$, $B_{\mathrm{m}p} \in \mathbb{R}^{n\times q}$ are constant *known* matrices with $A_{\mathrm{m}p} \in \mathbb{R}^{n\times n}$ Hurwitz matrices for $p \in \mathscr{N}$. We suppose that each pair $(A_{\mathrm{m}p},\ B_{\mathrm{m}p})$ is associated to its own corresponding subsystem (A_p, B_p) in (3-1). The following assumptions are made in order to have a well-posed adaptive problem:

Assumption 4. *There exist constant matrices $K^*_{\mathrm{x}p} \in \mathbb{R}^{n\times q}$ and invertible constant matrices $K^*_{\mathrm{r}p} \in \mathbb{R}^{q\times q}$ such that*

$$A_{\mathrm{m}p} = A_p + B_p {K^*_{\mathrm{x}p}}^T,\quad B_{\mathrm{m}p} = B_p K^*_{\mathrm{r}p}. \tag{3-3}$$

Assumption 5. *There exist known matrices $S_p \in \mathbb{R}^{q\times q}$ such that*

$$\Gamma_p = K^*_{\mathrm{r}p} S_p \tag{3-4}$$

are positive definite.

Assumption 6. *For each subsystem in (3-1), the matrices A_p and B_p belong to a known and bounded uncertainty set Θ_p.*

Remark 5. *Assumptions 4 and 5 are the generalization of Assumptions 1 and 2 for switched systems. Assumption 6 is required to obtain a bound on the increasing rate of the tracking error during the zooming-out phase, as it will be illustrated in Section 3-3.*

Since A_p and B_p are unknown in (3-1), the control gains $K^*_{\mathrm{x}p} \in \mathbb{R}^{n\times q}$ and $K^*_{\mathrm{r}p} \in \mathbb{R}^{n\times q}$ in (3-3) must be estimated. In the spirit of [4], the following switched adaptive controller is applied:

$$u(t) = K^T_{\mathrm{x}\sigma(t)}(t)x(t) + K_{\mathrm{r}\sigma(t)}(t)r(t),\ \sigma(t) \in \mathscr{N} \tag{3-5}$$

where $K_{\mathrm{x}p}$, $K_{\mathrm{r}p}$, $p \in \mathscr{N}$, are the estimates of $K^*_{\mathrm{x}p}$, $K^*_{\mathrm{r}p}$ respectively, to be updated by an appropriate adaptive law to be introduced in the next section. We consider a networked control setup with the controller on the sensor side, so that the control input given by (3-5) must be quantized and sent to the actuator via a communication channel. The quantizer is given by (2-8), with u given by (3-5), and η given by $\eta = K^T_{\mathrm{x}p}x_{\mathrm{m}} + K_{\mathrm{r}p}$. Our control objective is formulated as follows:

3-1-2 Problem formulation

Problem 2. ***(Input-quantized switched linear model reference adaptive control)**: Design an adaptive control law for the control gains in (3-5), and adjustment strategies for the dynamic parameter μ and dynamic offset η in (2-8) such that, without requiring the knowledge of A_p and B_p in (3-1), the state trajectories of the uncertain switched system (3-1) track asymptotically the trajectories generated by the switched reference model (3-2).*

3-2 Adaptive law controller design

In order to guarantee that the states x in (3-1) track x_{m} in (3-2) asymptotically, we need first to guarantee global asymptotic stability of the homogeneous part of the reference switched system (3-1) (i.e. with $r = 0$) under a dwell-time admissible switching law $\sigma(\cdot) \in \mathscr{D}(\tau_d)$. Inspired by [34], [30], the following lemma is stated.

Lemma 3-2.1. *The homogeneous part of the reference switched system (3-2) is globally asymptotically stable for any switching law $\sigma(\cdot) \in \mathscr{D}(\tau_d)$ if there exist: a collection of symmetric matrices $P_{p,c} \in \mathbb{R}^{n\times n}$, $p \in \mathscr{N}$, $c = 0, 1, ..., C$, and a sequence $\{\delta_c\}_{c=1}^{C} > 0$ with $\sum_{c=1}^{C} \delta_c = \tau_d$ such that the following holds:*

$$P_{p,c} > 0 \tag{3-6a}$$

$$\frac{P_{p,c+1} - P_{p,c}}{\delta_{c+1}} + P_{p,c}A_{\mathrm{m}p} + A_{\mathrm{m}p}^T P_{p,c} < 0 \tag{3-6b}$$

$$\frac{P_{p,c+1} - P_{p,c}}{\delta_{c+1}} + P_{p,c+1}A_{\mathrm{m}p} + A_{\mathrm{m}p}^T P_{p,c+1} < 0 \tag{3-6c}$$

$$c = 0, ..., C-1$$

$$P_{p,C}A_{\mathrm{m}p} + A_{\mathrm{m}p}^T P_{p,C} < 0 \tag{3-6d}$$

$$P_{p,C} - P_{l,0} \geq 0 \tag{3-6e}$$

$$\forall l = 1, ..., p-1, p+1, ...N,$$

where C is a positive integer that can be selected a priori, depending on the allowed computational complexity.

By solving the linear matrix inequalities (LMIs) in (3-6), we obtain a collection of symmetric matrices $P_{p,c}$. This collection of matrices is used to obtain a time varying matrix $P_p(t)$ via interpolation. The time-varying matrix $P_p(t)$, $p \in \mathscr{N}$ is defined as:

$$P_p(t) = \begin{cases} P_{p,c} + \frac{P_{p,c+1}-P_{p,c}}{\delta_{c+1}}(t - t_{i,c}), & \text{for } t_{i,c} \leq t < t_{i,c+1} \\ P_{p,C} & \text{for } t_{i,C} \leq t < t_{i+1} \end{cases} \tag{3-7}$$

and it will be used later to define and an appropriate Lyapunov function. Assume that $\sigma(t_i) = p$ and $\sigma(t_{i+1}) = l$, with $i \in \mathbb{N}^+$ and $p, l \in \mathscr{N}$. By defining a time sequence $\{t_{i,0}, ..., t_{i,C}\}$ with $t_{i,c+1} - t_{i,c} = \delta_{c+1}$, $c = 0, ..., C-1$, and assuming $t_{i,0} = t_i$, $t_{i,C} - t_i = \tau_d$, the time sequence between two switching instants t_i, t_{i+1} (and corresponding matrices $P_{p,c}$) can be seen in Fig. 3-1. The dashed vertical lines denote the value of $P_p(t)$ at each corresponding time instant.

When the quantized adaptive state-feedback controller given by (2-8) is applied to (3-1), the closed-loop system reads as:

$$\begin{aligned} \dot{x}(t) =& A_{\sigma(t)}x(t) + B_{\sigma(t)}\left(K_{\mathrm{x}\sigma(t)}^T x(t) + K_{\mathrm{r}\sigma(t)}r(t)\right) \\ &+ B_{\sigma(t)}\mu \underbrace{\left[g\left(\frac{K_{\mathrm{x}\sigma(t)}^T x(t) + K_{\mathrm{r}\sigma(t)}r(t) - \eta(t)}{\mu}\right) - \frac{K_{\mathrm{x}\sigma(t)}^T x(t) + K_{\mathrm{r}\sigma(t)}r(t)}{\mu}\right]}_{\Delta_{\mathrm{u}}} \end{aligned} \tag{3-8}$$

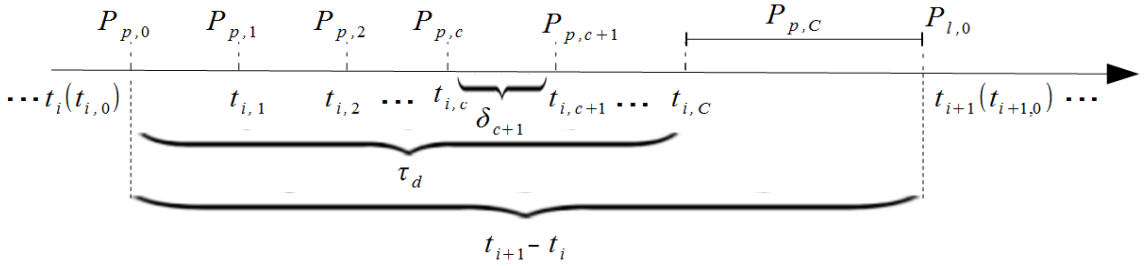

Figure 3-1: Time sequence and values of $P_p(t)$ between two switching instants t_i, t_{i+1}.

where in case of no saturation, it holds from (1-2), $\|\Delta_{\mathrm{u}}\| \leq \Delta$. In view of (3-2) and (3-8), the evolution of the tracking error can be written as

$$\dot{e}(t) = \dot{x}(t) - \dot{x}_{\mathrm{m}}(t) = A_{\mathrm{m}\sigma(t)}e(t) + B_{\sigma(t)}\tilde{K}^T_{\mathrm{x}\sigma(t)}x(t) + B_{\sigma(t)}\tilde{K}_{\mathrm{r}\sigma(t)}r(t) + B_{\sigma(t)}\mu\Delta_{\mathrm{u}} \tag{3-9}$$

where $\tilde{K}_{\mathrm{x}p} = K_{\mathrm{x}p} - K^*_{\mathrm{x}p}$, $\tilde{K}_{\mathrm{r}p} = K_{\mathrm{r}p} - K^*_{\mathrm{r}p}$, $p \in \mathscr{N}$, are defined as the controller parameter errors.

In order to analyze the stability of the closed-loop system (3-9) the following Lyapunov-like function is considered:

$$V(t) = e(t)^T P_{\sigma(t)}(t)e(t) + \sum_{p=1}^{N} tr\left[\tilde{K}_{\mathrm{x}p}(t)\Gamma_p^{-1}\tilde{K}^T_{\mathrm{x}p}(t)\right] + \sum_{p=1}^{N} tr\left[\tilde{K}^T_{\mathrm{r}p}(t)\Gamma_p^{-1}\tilde{K}_{\mathrm{r}p}(t)\right] \tag{3-10}$$

with $\Gamma_p \in R^{n\times n} > 0$ coming from (3-4).

In view of Assumption 6, lower and upper bounds for the controller parameters $K_{\mathrm{x}p}$, $K_{\mathrm{r}p}$ can be found (this can be done by testing the matching conditions (3-3) over the uncertainty set Θ_p, $\forall p \in \mathscr{N}$). The parameter projection adaptive law is derived as follows:

$$\begin{aligned} \dot{K}^T_{\mathrm{x}\sigma(t)}(t) &= -S^T_{\sigma(t)}B^T_{\mathrm{m}\sigma(t)}P_{\sigma(t)}(t)e(t)x(t)^T + F^T_{\mathrm{x}\sigma(t)} \\ \dot{K}_{\mathrm{r}\sigma(t)}(t) &= -S^T_{\sigma(t)}B^T_{\mathrm{m}\sigma(t)}P_{\sigma(t)}(t)e(t)r(t)^T + F_{\mathrm{r}\sigma(t)} \end{aligned} \tag{3-11}$$

where $F_{\mathrm{x}p}$ and $F_{\mathrm{r}p}$ are the projection terms that keep the estimates inside the lower and upper bounds, similarly to (2-19).

Remark 6. *The adaptive law (3-11) is implemented as follows: Let $\{t^+_{p_1}, t^+_{p_2}, ...\}$ represent the sequence of switch-in time instants of subsystem p, $p \in \mathscr{N}$, and let $\{t^-_{p_1}, t^-_{p_2}, ...\}$ represent the switch-out time instants of subsystem p. The initial conditions of (3-11) at a switch-in time instant for subsystem p are taken from the estimates at the previous switch-out time instant of the corresponding subsystem, thus it holds $K_{\mathrm{x}p}(t^+_{p_{k+1}}) = K_{\mathrm{x}p}(t^-_{p_k})$ and $K_{\mathrm{r}p}(t^+_{p_{k+1}}) = K_{\mathrm{r}p}(t^-_{p_k})$, $\forall k \in \mathbb{N}^+$. Subsequently, $K_{\mathrm{x}p}$, $K_{\mathrm{r}p}$ evolve continuously in time.*

It can be seen by (3-7) that, $P_{\sigma(\cdot)}(\cdot)$ is continuous in the time interval between two consecutive switches and discontinuous at switching time instants. Because the controller parameter estimates evolve continuously in time in view of Remark 6, $V(t)$ in (3-10) is continuous during the interval between two consecutive time instants and discontinuous at switching instants.

3-2-1 Stability with slow switching

We consider a time interval during two consecutive switching instants t_i and t_{i+1}, such that $\sigma(t_i) = p$ and $\sigma(t_{i+1}) = l$, with $i \in \mathbb{N}^+$ and $p, l \in \mathscr{N}$. For $t \in [t_i, t_{i+1})$, subsystem p is active and consequently $K_{\mathrm{x}j}$, $K_{\mathrm{r}j}$, $\forall j \in \mathscr{N}/p$, are kept constant with their values identified with the values at the last switch-out instant of subsystem j, before the switching instant t_i.

Using (3-11) and the properties of the projection terms $F_{\mathrm{x}p}$, $F_{\mathrm{r}p}$ [49], the time derivative of (3-10) along (3-9) is, during the interval $[t_i, t_{i+1})$:

$$\dot{V} = e^T \underbrace{\left(A_{\mathrm{m}p}^T P_p + P_p A_{\mathrm{m}p} + \dot{P}_p\right)}_{-Q_p} e + \underbrace{2tr\left[\tilde{K}_{\mathrm{x}p}\Gamma_p^{-1}F_{\mathrm{x}p}^T + \tilde{K}_{\mathrm{r}p}\Gamma_p^{-1}F_{\mathrm{r}p}\right]}_{K_{\mathrm{v}p}} + 2e^T P_p B_p \mu \Delta_{\mathrm{u}}, \quad (3\text{-}12)$$

and because $K_{\mathrm{v}p} \leq 0$ [49], (3-12) becomes

$$\dot{V} \leq -e^T Q_p e + 2e^T P_p B_p \mu \Delta_{\mathrm{u}}. \quad (3\text{-}13)$$

Because $K_{\mathrm{x}p}$, $K_{\mathrm{r}p}$ are bounded due to the projection terms in (3-11) we can define $\rho' \in \mathbb{R} \geq 0$ such that:

$$\rho' = \max_{t \geq 0} \sum_{p=1}^{N} \left\{ tr\left[\tilde{K}_{\mathrm{x}p}\Gamma_p^{-1}\tilde{K}_{\mathrm{x}p}^T\right] + tr\left[\tilde{K}_{\mathrm{r}p}^T\Gamma_p^{-1}\tilde{K}_{\mathrm{r}p}\right] \right\} \quad (3\text{-}14)$$

and because of (3-10) we have

$$e^T P_p e \leq V \leq e^T P_p e + \rho'. \quad (3\text{-}15)$$

Next, we analyze the properties of $-Q_p(t)$ in (3-13).

For $t \in [t_i, t_{i+1})$ we consider $t \in [t_{i,c}, t_{i,c+1})$, $c = 0, ..., C-1$. By looking at the expression of P_p in (3-7), one can see that $-Q_p$ can be written, in the time interval under consideration, as follows:

$$\begin{aligned} -Q_p =& \lambda_1 \left[\frac{(P_{p,c+1} - P_{p,c})}{\delta_{c+1}} + P_{p,c}A_{\mathrm{m}p} + A_{\mathrm{m}p}^T P_{p,c} \right] \\ &+ \lambda_2 \left[\frac{(P_{p,c+1} - P_{p,c})}{\delta_{c+1}} + P_{p,c+1}A_{\mathrm{m}p} + A_{\mathrm{m}p}^T P_{p,c+1} \right] \end{aligned} \quad (3\text{-}16)$$

where $\lambda_1 = 1 - \frac{(t-t_{i,c})}{\delta_{c+1}}$, $\lambda_2 = \frac{(t-t_{i,c})}{\delta_{c+1}}$. It can be seen by (3-6b), (3-6c), that

$$-Q_p(t) < 0, \text{ for } t \in [t_{i,c}, t_{i,c+1}). \quad (3\text{-}17)$$

Next, we consider the interval $t \in [t_{i,C}, t_{i+1})$ for the case $t_{i+1} - t_i > \tau_d$. In this case, it is true $P_p(t) = P_{p,C}$ because of (3-7), and because of (3-6d) it holds

$$-Q_p(t) = A_{\mathrm{m}p}^T P_{p,C} + P_{p,C}A_{\mathrm{m}p} < 0, \ t \in [t_{i,C}, t_{i+1}). \quad (3\text{-}18)$$

Because of (3-17), (3-18), we have

$$-Q_p(t) < 0, \text{ for } t \in [t_i, t_{i+1}). \quad (3\text{-}19)$$

Let $\sigma(t_i) = p$ and $\sigma(t_{i+1}) = l$ with $i \in \mathbb{N}^+$ and $p, l \in \mathscr{N}$. At the switching instant t_{i+1}, the following holds

$$V(t_{i+1}) - V(t_{i+1}^-) = e^T(t_{i+1})(P_{\sigma(t_{i+1})} - P_{\sigma(t_{i+1}^-)})e^T(t_{i+1}) = e^T(t_{i+1})(P_{l,0} - P_{p,C})e(t_{i+1})$$

and because of (3-6e), it must be true

$$V(t_{i+1}) - V(t_{i+1}^-) \leq 0. \tag{3-20}$$

Because $K_{\mathrm{x}p}$, $K_{\mathrm{r}p}$ and e evolve continuously with respect to the time, (3-20) states that the Lyapunov-like function V as given in (3-10) is non-increasing at switching time instants.

3-3 Hybrid control policy

Because of (3-19), it must be true that

$$\lambda_{min}(Q_p)\|e\|^2 \leq e^T Q_p e \leq \lambda_{max}(Q_p)\|e\|^2\,,\ p \in \mathscr{N},\ t \in [t_i, t_{i+1}), \tag{3-21}$$

where $\lambda_{max}(Q_p) \geq \lambda_{min}(Q_p) > 0$.

By referring to (3-13) and by assuming no saturation in the quantizer ($\|\Delta_{\mathrm{u}}\| \leq \Delta$), we are in a position to state the following:

$$\begin{aligned}\dot{V} &\leq -\lambda_{min}(Q_p)\|e\|^2 + 2e^T P_p B_p \mu\Delta \\ &\leq -\lambda_{min}(Q_p)\|e\| \left(\|e\| - \underbrace{\frac{2\max\limits_{B_p\in\Theta}\|P_pB_p\|}{\lambda_{min}(Q_p)}}_{R_p} \right) \implies\end{aligned}$$

$$\dot{V} \leq -\phi\|e\| \left(\|e\| - R'\mu\Delta \right) \tag{3-22}$$

with $\phi = \min\limits_{p\in\mathscr{N}}[\lambda_{min}(Q_p)]$, $R' = \max\limits_{p\in\mathscr{N}} R_p$, where R' is bounded in view of Assumption 6. According to (2-9), the requirement for no saturation can be equivalently expressed by the following condition:

$$\|u - \eta\| \leq \mu M. \tag{3-23}$$

We define

$$K_{\mathrm{x}}{}' = \max_{p\in\mathscr{N},\ t\geq 0} \left\| K_{\mathrm{x}p} \right\|. \tag{3-24}$$

Because $\|u - \eta\| = \left\| K_{\mathrm{x}p}^T x + K_{\mathrm{r}p} r - K_{\mathrm{x}p}^T x_{\mathrm{m}} - K_{\mathrm{r}p} r \right\| = \left\| K_{\mathrm{x}p}^T e \right\|$, the condition for no saturation is satisfied if the following condition is true:

$$\|e\| \leq \frac{\mu M}{K_{\mathrm{x}}{}'}, \tag{3-25}$$

We define

$$\min_{p\in\mathscr{N}}[\lambda_{min}(P_p)] = \xi_{min},\quad \max_{p\in\mathscr{N}}[\lambda_{max}(P_p)] = \xi_{max} \tag{3-26}$$

and the following regions:

$$\mathscr{B}_1{}'(\mu) := \left\{ e(t) : \|e(t)\| \leq \frac{\mu M}{K_{\mathrm{x}}{}'} \right\} \tag{3-27a}$$

$$\mathscr{I}_1{}'(\mu) := \left\{ e(t) : e(t)^T P_{\sigma(t)}(t) e(t) \leq \xi_{min} \frac{\mu^2 M^2}{K_{\mathrm{x}}{}'^2} \right\} \tag{3-27b}$$

$$\mathscr{B}_2{}'(\mu) := \left\{ e(t) : \|e(t)\| \leq \mu R' \Delta \right\} \tag{3-27c}$$

$$\mathscr{I}_2{}'(\mu) := \left\{ e(t) : e^T(t) P_{\sigma(t)}(t) e(t) \leq \xi_{max} \mu^2 R'^2 \Delta^2 \right\}. \tag{3-27d}$$

One can see that, if

$$\frac{\sqrt{\xi_{min}} M}{K_{\mathrm{x}}{}'} > \sqrt{\xi_{max}} R' \Delta$$

then it holds $\forall P_{\sigma(t)}(t)$, $\sigma(t) \in \mathscr{N}$, $t \geq 0$: $\mathscr{B}_2{}'(\mu) \subset \mathscr{I}_2{}'(\mu) \subset \mathscr{I}_1{}'(\mu) \subset \mathscr{B}_1{}'(\mu)$.

3-3-1 Main result

Using similar argumentation as in Theorem 2-3.1, the following theorem is proposed:

Theorem 3-3.1. *Consider the input-quantized model reference adaptive control given by the switched uncertain system (3-1), the switched reference model (3-2), the dynamic quantizer with adjustable offset (2-8), and the adaptive law (3-11). If the following condition holds*

$$\frac{\sqrt{\xi_{min}}M}{{K_{\mathrm{x}}}'} > \sqrt{\xi_{max}}R'\Delta \tag{3-28}$$

(with ξ_{min}, ξ_{max} be defined in (3-26), ${K_{\mathrm{x}}}'$ be defined in (3-24) and R' defined after (3-22)), then there exists an error-based hybrid quantized feedback control policy that renders the closed-loop system (3-9) globally asymptotically stable with $\lim_{t\to\infty} e(t) = 0$.

Proof. The hybrid quantized feedback policy is designed following a similar approach as the one proposed by Theorem 2-3.1. We distinguish two phases, the zooming-out and zooming-in phases. During zooming-out phase, we increase μ in such a way, so that to avoid saturation and during zooming-in phase, we shrink the smaller region $\mathscr{I}_2'(\mu)$ by reducing the hybrid parameter μ so that state-tracking properties can be concluded. The two phases are examined thoroughly as follows:

Zooming-out phase: Let $\mu(0) = 1$. If $\|e(0)\| > \frac{M}{{K_{\mathrm{x}}}'}$ we have saturation. In this case we make $\mu(t)$ increase in a piecewise fashion to dominate the growth of e, which it can be seen by (3-9) that equals $\left|e^{\max_{A_p,B_p\in\Theta}\|A_p+B_pK_{\mathrm{x}p}^T\|}\right|$ with $\max_{A_p,B_p\in\Theta}\left\|A_p + B_pK_{\mathrm{x}p}^T\right\|$ bounded in view of Assumption 6. There will be a time instant $t_0 \geq 0$ and a bounded $\mu(t_0)$ at which the following relation will be true:

$$\|e(t_0)\| \leq \sqrt{\frac{\xi_{min}}{\xi_{max}}}\frac{\mu(t_0)M}{{K_{\mathrm{x}}}'} \tag{3-29}$$

and as a consequence of (3-14), $e(t_0) \in {\mathscr{I}_1}'(\mu(t_0)) \cap {\mathscr{B}_1}'(\mu(t_0))$. Let us assume two consecutive switching time instants t_i and t_{i+1}, such that $\sigma(t_i) = p$, $\sigma(t_{i+1}) = l$, $p, l \in \mathscr{N}$. If $t_0 \in [t_i, t_{i+1})$, then it is true that, because $e(t_0) \in {\mathscr{B}_1}'(\mu(t_0))$ and $\mathscr{B}_2(\mu) \subset \mathscr{B}_1(\mu)$ from (3-28), by looking at the expression of $\dot{V}$ in (3-22), we get $\dot{V} \leq 0$.

One can see that, for $t \in [t_i, t_{i+1})$, $t \geq t_0$, when $e(t_0) \in {\mathscr{B}_1}'(\mu(t_0))$ and $\dot{V} \leq 0$, we have

$$V(t) \leq V(t_0) \implies \|e(t)\| \leq \sqrt{\frac{\mu^2(t_0)M^2}{{K_{\mathrm{x}}}'^2} + \frac{\rho'}{\xi_{min}}}. \tag{3-30}$$

Moreover, if $t = t_{i+1}$, because e evolves continuously, (3-30) still holds implying that $e(t)$ does not necessarily belong to ${\mathscr{B}_1}'(\mu(t_0))$. Hence, for $t \geq t_0$ there might be two cases: either the norm of the tracking error is decreasing and we go to the zooming-in phase; or the norm of the tracking error is increasing in which case we keep increasing $\mu(t)$ at the same rate to avoid saturation and guarantee that $e(t) \in {\mathscr{B}_1}'(\mu(t))$. For the second case, because $\mu(t)$ is updated at much higher rate compared to the growth of $e(t)$ to avoid saturation, we can assume that $\forall t \geq t_0 \implies e(t) \in {\mathscr{B}_1}'(\mu(t))$. Because from (3-20) we have that V is non-increasing at time-switching instants, if additionally in the time interval between two switchings $[t_i, t_{i+1})$

it holds $\forall t \geq t_0$, $e(t) \notin \mathscr{B}_2{}'(\mu(t))$, then it is true that $\dot{V}(t) \leq 0$, $\forall t \geq t_0$. In this case, because of (3-30), it is true $e(t) \in \mathscr{L}_\infty$, $\forall t \geq t_0$.

Zooming-in phase: Let t' be a time instant such that $t \geq t' \geq t_0$, and $e(t) \in \mathscr{B}_1{}'(\mu(t'))$. It is true, as it was shown in the zooming-out phase, that $\dot{V} \leq 0$ between time switching instants as long as $e \notin \mathscr{B}_2{}'(\mu(t'))$, and V is non increasing at switching time instants. Then, (3-30) holds implying $V(t)$ is bounded. One can see from (3-27) that $\mathscr{B}_2{}'(\mu) \subset \mathscr{I}_2{}'(\mu)$. Thus, at time $\tilde{t}$ with $\tilde{t} \geq t'$, if $e(t) \in \mathscr{I}_2{}'(\mu(t'))$, $\mu(\tilde{(t)})$ is updated

$$\mu(\tilde{t}) = \underbrace{\frac{K_{\mathrm{x}}{}'\sqrt{\xi_{max}}R'\Delta}{\sqrt{\xi_{min}}M}}_{\Omega'}\mu(t'). \tag{3-31}$$

In view of (3-28) it holds $\Omega' < 1$. Then, zooming-in event occurs, and by looking at (3-27) one can see that $\mathscr{I}_1{}'(\mu(\tilde{t})) = \mathscr{I}_2{}'(\mu(t'))$, where $\mu(t')$ is the value of μ that prevents saturation (according to (3-29), with $\mu(t_0)$ replaced by $\mu(t')$). After the zooming-in event one might have two cases: either the tracking error increases tending to violate $e \in \mathscr{B}_1{}'(\mu(\tilde{t}))$, in which case a new zooming-out phase is activated; or the tracking error keeps decreasing in which case a new zooming-in event will eventually be triggered. In the second case, since μ is updated when $e \in \mathscr{I}_2{}'(\mu)$ and because $\mathscr{B}_2{}'(\mu) \subset \mathscr{I}_2{}'(\mu)$, it is true that $\dot{V} \leq 0$ during the time interval between two consecutive switchings, as it was proven in the zooming-out phase.

Let us now look at the combined behavior of zooming-in and zooming-out phases. For $t \geq t_0$, at both zooming-in and zooming-out phases, because V is not increasing it holds $V(t)$ is lower-bounded by $V(t_0)$. Moreover, because $\dot{V} < 0$ (for $\|e\| \neq 0$) between switching time instants if $e \notin \mathscr{B}_2{}'(\mu)$, and because V is non-increasing at switching time instants it is true that V is bounded. Because V is bounded, (3-30) holds implying $e(t) \in \mathscr{L}_\infty$, $\forall t \geq t_0$. By looking at (3-9) we can conclude with similar argumentation that $\dot{e}$ is bounded because it consists of bounded terms. Finally, by looking at the expression of $\dot{V}$ in (3-12), one can see that $\ddot{V}$ is bounded, as it consists of bounded terms, thus it is bounded in the interval between time switching instants. As a result of the generalized Barbalat's lemma, it holds that $\lim_{t\to\infty} \dot{V}(t) = 0$.

Consequently, the following relation from (3-22) holds:

$$\lim_{t\to\infty} \dot{V}(t) \leq -\phi\Big(\lim_{t\to\infty}\|e(t)\|\left(\|e\| - R'\mu\Delta\right)\Big) \implies$$
$$0 \leq -\phi\Big(\lim_{t\to\infty}\|e(t)\|\left(\|e\| - R'\mu\Delta\right)\Big).$$

The above relation is true when

$$\lim_{t\to\infty}\|e(t)\| = 0 \quad \text{or} \quad \lim_{t\to\infty}\|e(t)\| - \mu(t)R'\Delta \leq 0. \tag{3-32}$$

The second relation implies that $e \in \mathscr{B}_2{}'(\mu)$. However, when $e \in \mathscr{I}_2{}'(\mu)$, a zooming-in event occurs and because $\mathscr{B}_2{}'(\mu) \subset \mathscr{I}_2{}'(\mu)$ it is always true that $e \notin \mathscr{B}_2{}'(\mu)$. As a consequence $\lim_{t\to\infty} \mu(t) = 0$ and by (3-32) we conclude that $\lim_{t\to\infty}\|e(t)\| = 0$. Because all signals are bounded and $\lim_{t\to\infty} e(t) = 0$, we can conclude that (3-9) is globally asymptotically stable.

□

Remark 7. *The classical condition for asymptotic tracking using switching laws based on dwell time, as explained in the Lemma A-1.1 in the Appendix, assumes candidate Lyapunov functions satisfying inequalities of the form (A-6). This result is not applicable to our case due to the nature of V as expressed by the inequalities in (3-15). The most established results on adaptive control of switched systems, the switching laws based on dwell-time [36] or average dwell-time [50], assume a Lyapunov function with an exponential decay, during the interval between consecutive switches, i.e., $\dot{V} \leq -\alpha V - (V - m)$, for $V > m$, where α denotes a compatible number with $\alpha > 0$. Note that the switching laws based on this property and adaptive laws with constant positive definite matrices P_p prevent asymptotic tracking from being achieved.*

Remark 8. *In [41] a classic multiple quadratic Lyapunov function with a constant positive definite matrix was adopted. This implies that at every switching instant it was necessary to zoom out, in order to compensate the possible increment of the Lyapunov function at the switching time instants. Here, the time-varying Lyapunov function (3-10) we adopt is non-increasing at the switching instants, which does not require to zoom out (discontinuously) at each switching instant to compensate possible discontinuous increments (i.e. jumps). It might be necessary however to zoom-out (continuously) in case the activation of a new subsystem generates a transient in the tracking error (e.g. due to poor estimates of a subsystem that is activated for the first time). This mechanism, which gets rids completely of any discontinuous zooming-out phase, greatly simplifies the design of the dynamic quantizer and makes it consistent with the zooming procedure in non-switched systems [14].*

3-4 Summary

This work has established a novel adaptive control approach that attains asymptotic tracking for switched linear systems with parametric uncertainties and dwell-time switching with quantized input measurements. In addition to enlarging the class of systems for which the adaptive quantized control can be solved, we have also introduced a time-scheduled Lyapunov approach in an adaptive framework in order to avoid to zoom out at every switching instant to compensate the possible increment of the Lyapunov function at the switching instants. A Lyapunov-based approach has been used to derive the adaptive adjustments for the control parameters, and for the dynamic range and dynamic offset of the quantizer: the resulting (error-dependent) hybrid control policy has been given in a constructive manner, and asymptotic state tracking was shown. A practical example of the NASA GTM model will be used in Section 4-2 in order to demonstrate the effectiveness of the proposed hybrid adaptive control scheme.

Chapter 4

Simulation results

This Chapter is organized as follows: In Section 4-1, the effectiveness, stability and tracking properties of the quantized adaptive hybrid control methodology studied in Section 2-3, is verified via simulations. A networked implementation of the proposed design using an encoding/decoding scheme is shown in Subsection 4-1-3. In Section 4-2, the hybrid control policy studied in Section 2-3 and the adaptive law using the time scheduled Lyapunov function from Section 3-3 are used to evaluate, via simulations, the tracking performance for the case of unknown switched linear systems driven by a dwell-time switching policy.

4-1 Quantized adaptive control: an electro-hydraulic system test case

In this section we study the effectiveness of the adaptive hybrid control policy studied in Section 2-3 using the electro-hydraulic system studied in [49], [51].

4-1-1 Design and simulation parameters

The system shown in Fig. 4-1, consists of a Moog E760 torque motor/flapper operated four-way double-acting servovalve, hydraulically connected to a cylinder/actuator arm. The actuator cylinder has a diameter of 32 m, the actuator arm has a stroke of approximately l00 mm and the end of the arm is connected to an inertial load representing an aircraft control surface.

The operating condition with respect to supply pressure 11.0 MPa is selected, and the corresponding transfer function is:

$$G(s) = \frac{62.4}{s(s + 4.58)}$$

which can be equivalently written in controllable canonical form:

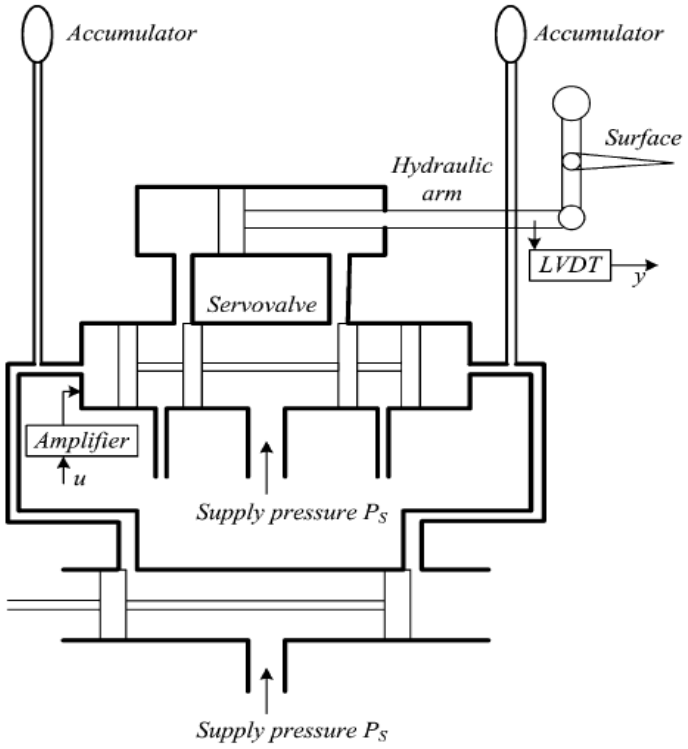

Figure 4-1: A schematic diagram of the electro-hydraulic system

$$\dot{x}(t) = \begin{bmatrix} 0 & 1 \\ 0 & -4.58 \end{bmatrix} x(t) + \begin{bmatrix} 0 \\ 62.4 \end{bmatrix} u(t) \tag{4-1}$$

where $x = [x_1, x_2]^T$, with x_1, x_2 representing the displacement and the velocity of the arm respectively, $u(t)$ is the control voltage and $y(t)$ is the measurement of the actuator arm displacement.

The desired dynamics are given as follows:

$$\dot{x}_{\mathrm{m}}(t) = \begin{bmatrix} 0 & 1 \\ -15 & -8 \end{bmatrix} x_{\mathrm{m}}(t) + \begin{bmatrix} 0 \\ 31.2 \end{bmatrix} r(t)$$

where the reference input signal $r(t)$ is specified as $r(t) = \sin(0.8\pi t) + \sin(\pi t)$. Moreover, the matrices P, Q in (2-11) are defined as

$$P = \begin{bmatrix} 1.2830 & 0.1030 \\ 0.1030 & 0.0578 \end{bmatrix}, \quad Q = \begin{bmatrix} 2.1811 & 0.1751 \\ 0.1751 & 0.0983 \end{bmatrix}$$

and S in (2-4) is chosen equal to 2. The quantizer is chosen so that $M = 10$, $\Delta = 0.01$ and μ initially is 1. The initial error in the simulations is chosen $e(t_0) = [0.1, -0.2]^T$. The controller parameters are assumed to reside between lower and upper bounds as follows: $K_{\mathrm{r}} \in [0.01, 0.8]$, $K_{\mathrm{x}}^{(i,j)} \in [-0.5, 0.5]$, $i, j = \{1, 2\}$ (the notation $K^{(i,j)}$ represents the (i, j)-th entry of matrix K). The initial parameter estimates are chosen $K_{\mathrm{x}}(0) = \begin{bmatrix} 0 & 0 \end{bmatrix}$, $K_{\mathrm{r}}(0) = 0.6$.

4-1-2 Simulation results

At first, we present the simulation results in Matlab-Simulink® for the case of no input quantization: tracking performance is shown in Fig. 4-2, while parameter estimates in Fig. 4-3.

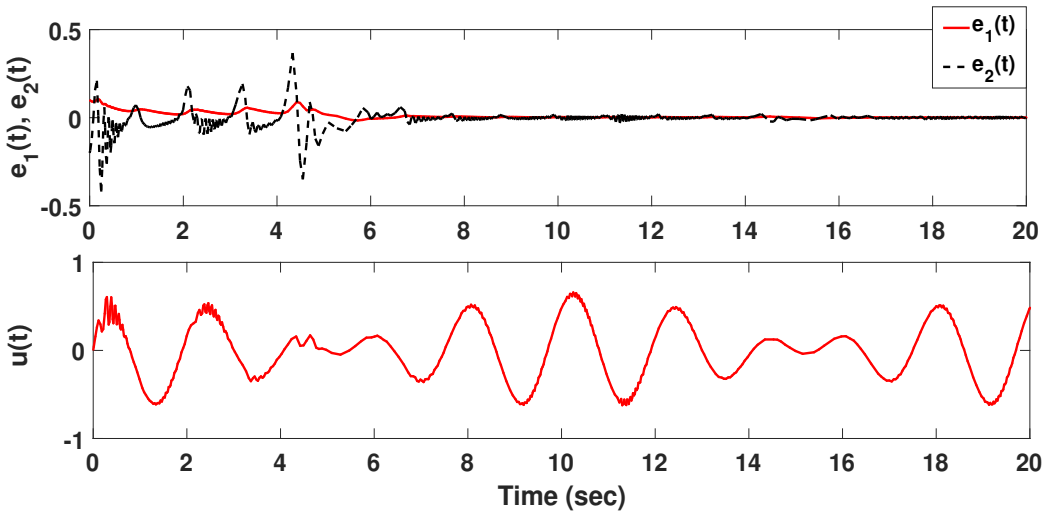

Figure 4-2: State tracking error and control input without input quantization

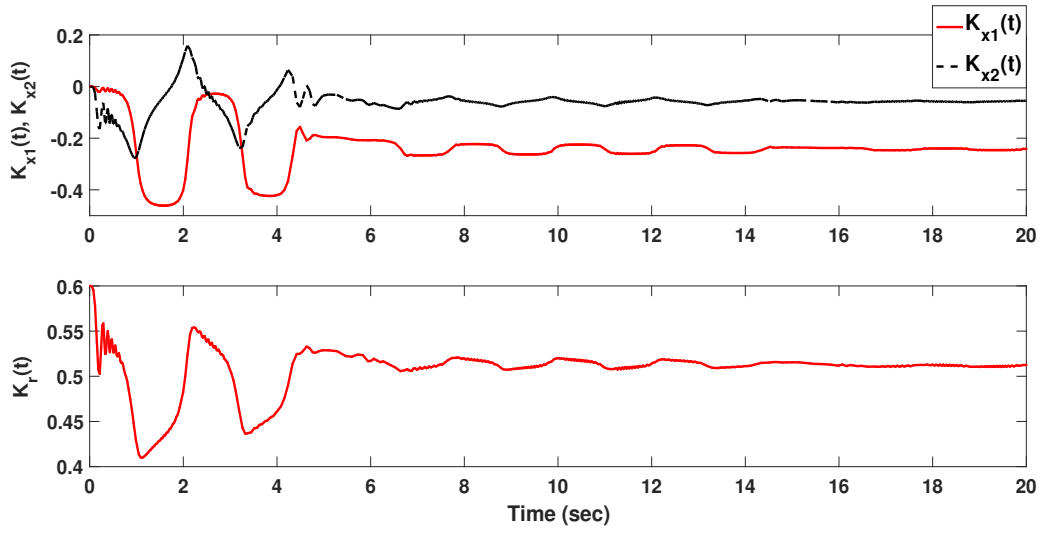

Figure 4-3: Controller parameters without input quantization

Next, we perform similar simulations for the case of dynamic input quantizer with adjustable offset. For the purpose of the simulation Ω in (2-40) is computed $\Omega = 0.78$.

Fig. 4-4 and Fig. 4-5 shows that the tracking performance of the dynamic quantizer with adjustable offset is clearly satisfactory: it is hard to notice any difference among Fig. 4-2 – Fig. 4-3 (no quantization) and Fig. 4-4 – Fig. 4-5 (dynamic quantization). This reveals that the same tracking performance can be attained without the need for infinite bandwidth.

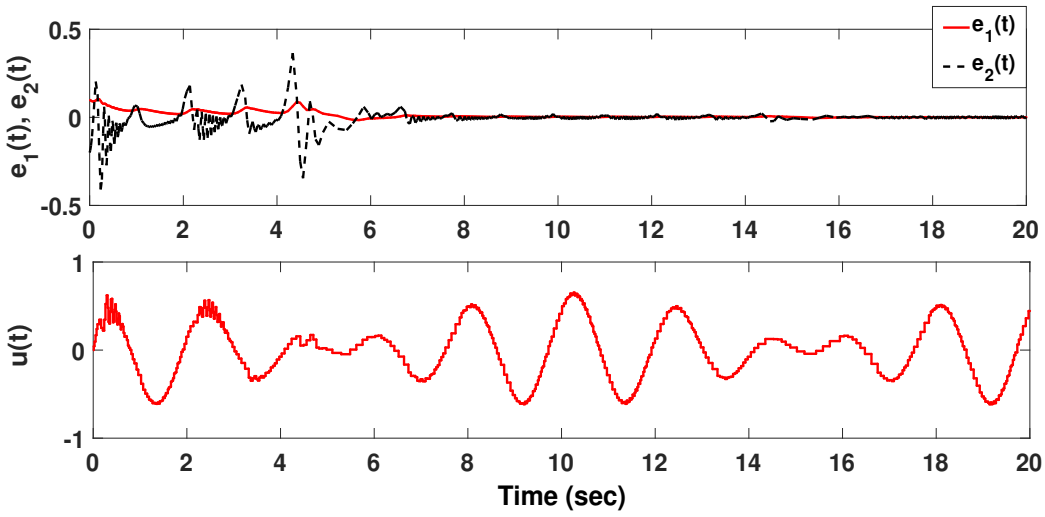

Figure 4-4: State tracking error and control input with input quantization

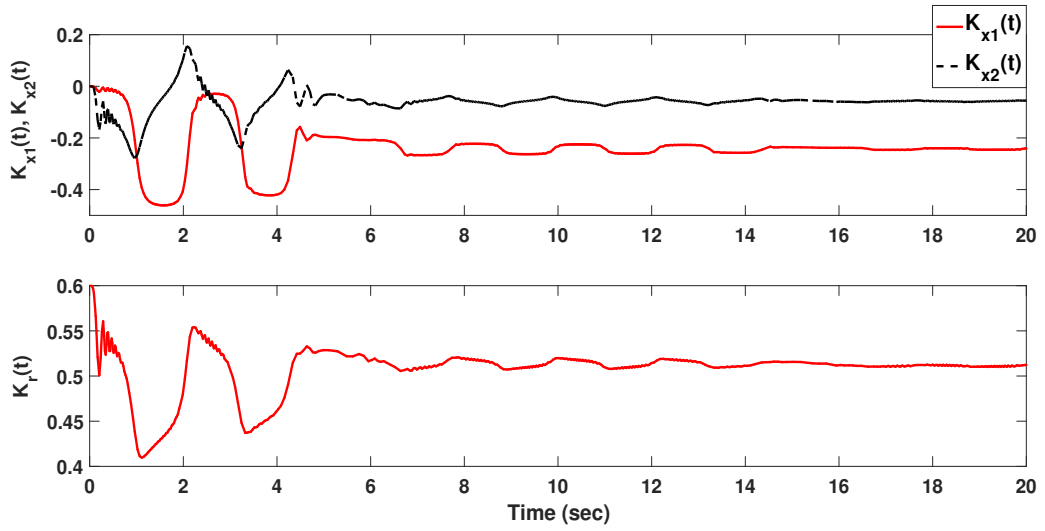

Figure 4-5: Controller parameters with input quantization

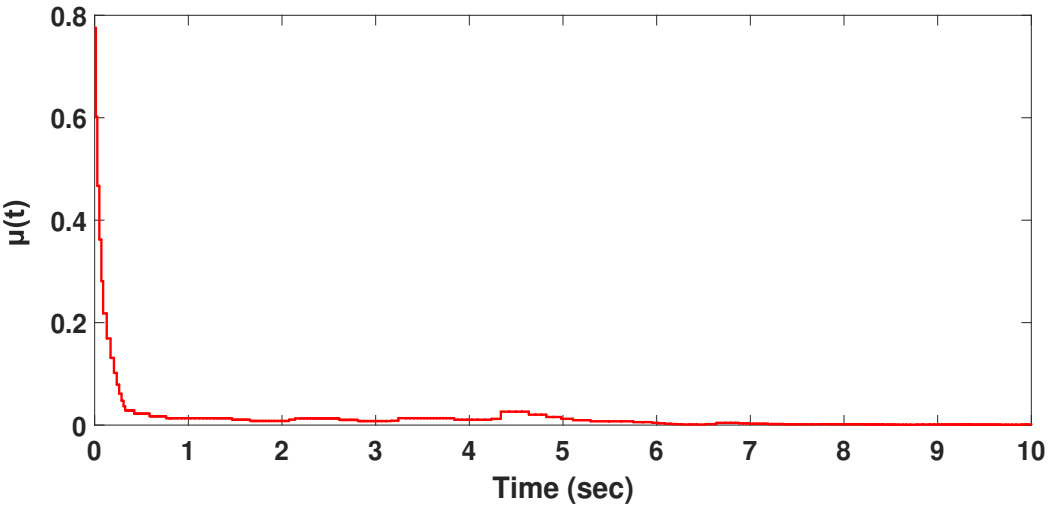

Figure 4-6: Hybrid control parameter $\mu(t)$ versus time (for the first 10 seconds of the simulation)

Details about the implementation of the proposed quantizer (including encoder and decoder) are given in subsection 4-1-3.

The parameter μ in Fig. 4-6 is decreasing abruptly since the first seconds of the experiment, indicating that the condition $e \in \mathscr{I}_2(\mu)$ triggers (2-40) very often and state-tracking is achieved quite fast. Because μ stays close to 0, from (2-10) we have that the quantized measurement of the input $g_{\eta\mu}(u)$ is almost identical to the actual input value u, thus it holds $g_{\eta\mu}(u) \approx \eta = K_{\mathrm{x}}^T x_{\mathrm{m}} + K_{\mathrm{r}} r$, which is the desired input value to achieve asymptotic state-tracking in the non-quantized model reference adaptive control case.

One can see in Fig. 4-6 that μ is not strictly decreasing, indicating intermediate zooming-out phases in between zooming-in time intervals which complies with our theoretical result in (2-38). When $e \notin \mathscr{B}_1(\mu)$, μ is increased continuously in a piecewise fashion faster than the growth of $\|e\|$ to avoid saturation. Then μ decreases in a piecewise manner when $e \in \mathscr{I}_2(\mu)$, according to (2-40), and subsequently new smaller regions $\mathscr{I}_1(\mu)$, $\mathscr{I}_2(\mu)$ are obtained.

4-1-3 Networked implementation of the dynamic quantizer

In this section we investigate the applicability of the proposed hybrid adaptive control design in the framework of networked control systems. In particular, for the simulations in Section 4-1, we implemented the encoding/decoding scheme shown in Fig. 4-7.

The decoder located on the actuator side waits for the quantized values of μ, η and the quantization level associated to the dynamic quantizer $g_{\eta\mu}(u)$, so that it can reconstruct the input u computed by the adaptive controller. In order to encode μ and η, we designed uniform static quantizers with dynamic range $M = 10$ and quantization error $\Delta = 0.001$, thus we need to transmit 20001 quantization levels (encoded in 15 bits). The decoder maps the received bits into the associated quantization level, for μ, η and $g_{\eta\mu}(u)$. The transmitter is event-triggered, i.e. no data packages (15 bits for μ, η or 11 bits for $g_{\eta\mu}(u)$) are sent till a switch to a new quantization level occurs. Fig. 4-8 shows the bit depth (number of bits of information) transmitted at each triggered transmission time instant for μ, η and $g_{\eta\mu}(u)$.

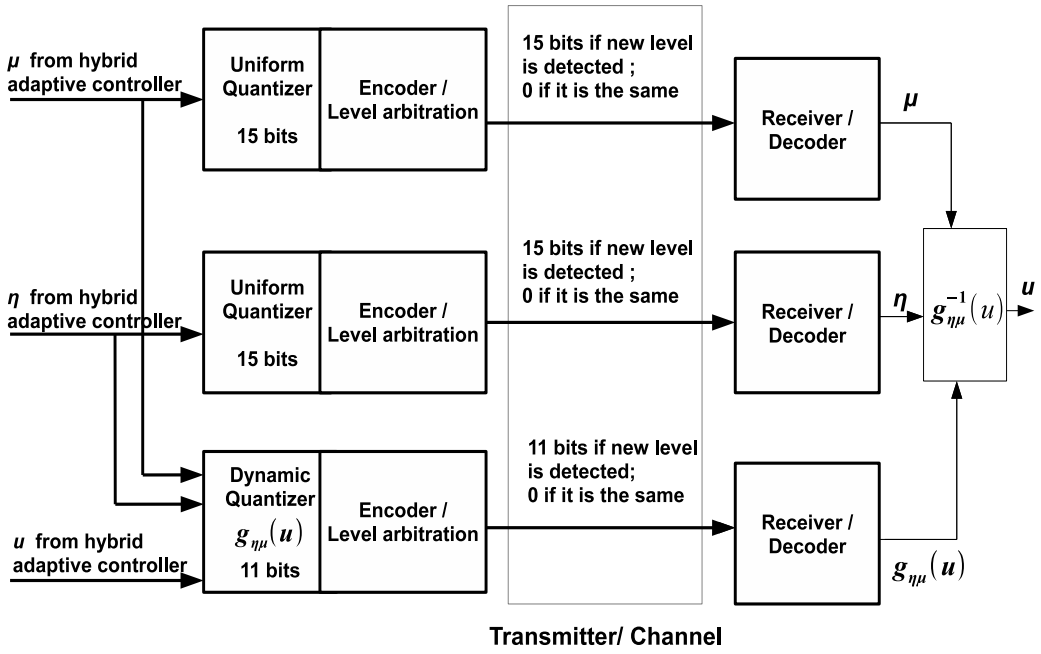

Figure 4-7: Block diagram of the implemented encoding/decoding scheme

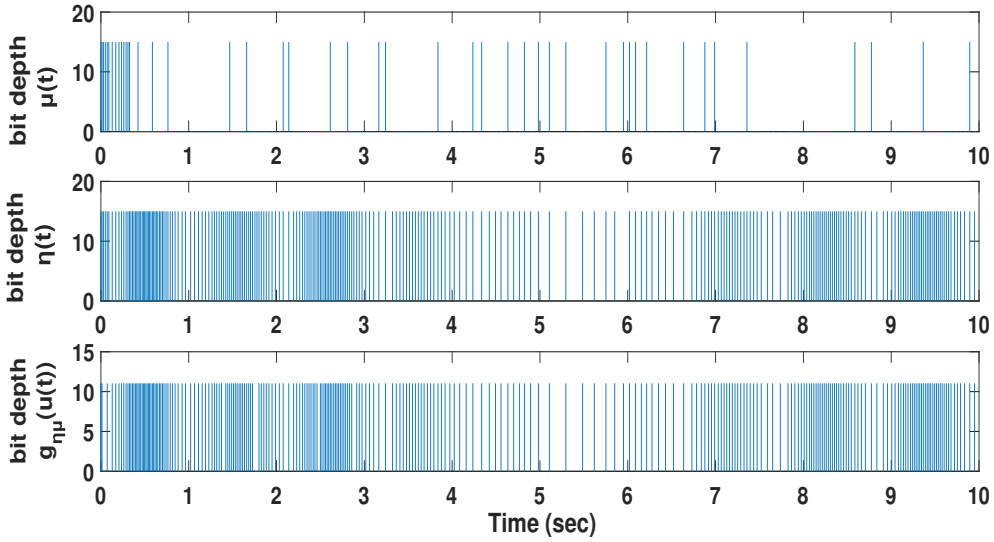

Figure 4-8: Bit depth for μ, η and $g_{\eta\mu}(u)$ (for the first 10 seconds of the simulation)

The transmission of μ is activated less often (mostly during zooming-out phases) because, as shown in Subsection 4-1-2, μ approaches zero very fast. Finally, the bit rate (the number of bits per second transmitted through the network) is illustrated in Fig. 4-9, where it can be seen that the maximum bit rate is around 3 Kbit/s.

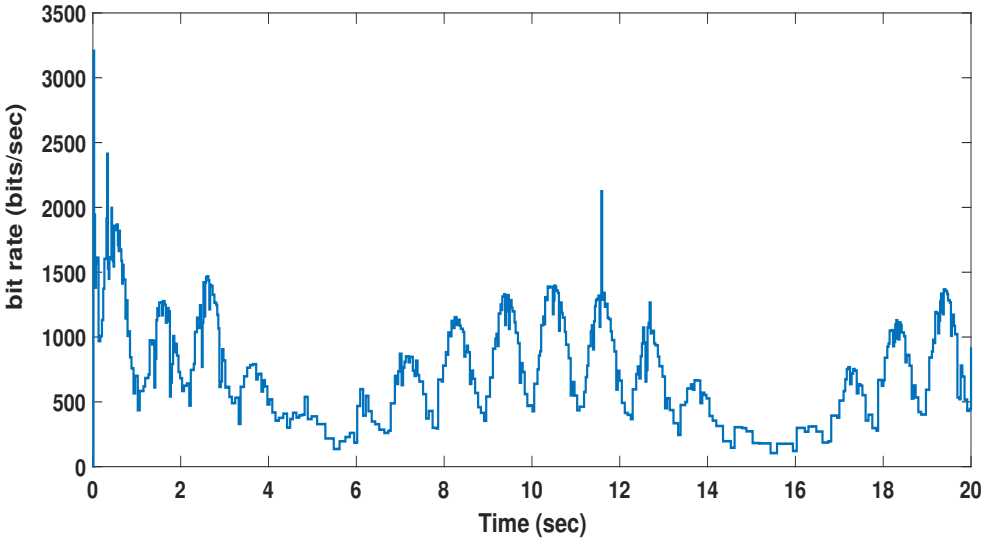

Figure 4-9: Transmitted bit rate

4-2 Quantized adaptive control of piecewise linear systems: a NASA GTM test case

In this section we study the effectiveness of the proposed adaptive hybrid control policy, performed on the NASA Generic Transport Model (GTM) [52].

4-2-1 Design and simulation parameters

The system, is linearized at steady-state, straight, wings-level flight condition at 75 and 85 kt at 800 ft, respectively. More precisely, the GTM models linearized at points $x_{01} = [127.6597, 10.3615, 0, 8.0987]^T$, $u_{01} = [1.3109, 14.1457]^T$ and $x_{02} = [144.9022, 8.5931, 0, 5.9234]^T$, $u_{02} = [2.3649, 14.8592]^T$, are given respectively as follows:

$$A_1 = \begin{bmatrix} -0.0190 & 0.0825 & -0.1005 & -0.3206 \\ -0.2154 & -2.7859 & 1.2031 & -0.0271 \\ 3.2527 & -30.7871 & -3.5418 & 0 \\ 0 & 0 & 1 & 0 \end{bmatrix}, \; B_1 = \begin{bmatrix} 0.0065 & 0.0534 \\ -0.6103 & 0.0020 \\ -74.6355 & 0.5431 \\ 0 & 0 \end{bmatrix}$$

$$A_2 = \begin{bmatrix} -0.0312 & 0.1095 & -0.0938 & -0.3210 \\ -0.1057 & -3.2245 & 1.3765 & -0.0217 \\ 3.9602 & -33.8308 & -4.0756 & 0 \\ 0 & 0 & 1 & 0 \end{bmatrix}, \; B_2 = \begin{bmatrix} 0.0032 & 0.0534 \\ -0.7821 & 0.0020 \\ -96.0149 & 0.5431 \\ 0 & 0 \end{bmatrix}$$

and the desired dynamics are given as follows:

$$A_{m1} = \begin{bmatrix} -0.0215 & 0.0810 & -0.0988 & -0.3180 \\ -0.0706 & -2.6377 & 1.0345 & -0.2636 \\ 20.9585 & -12.6579 & -24.1637 & -28.9269 \\ 0 & 0 & 1 & 0 \end{bmatrix}$$

$$A_{m2} = \begin{bmatrix} -0.0328 & 0.1088 & -0.0930 & -0.3196 \\ 0.0753 & -3.0601 & 1.1577 & -0.3276 \\ 26.1845 & -13.6389 & -30.9393 & -37.5452 \\ 0 & 0 & 1 & 0 \end{bmatrix}$$

with $B_{m1} = B_1$ and $B_{m2} = B_2$ for the reference model. It is important to underline that the matrices A_1, B_1, A_2, B_2 are given for simulation purposes, while the controller design does not use the knowledge of these matrices (only the knowledge of the reference model is used). The matrices S_p, $p = 1, 2$, in (3-11) are chosen as $S_1 = S_2 = 0.05 \cdot I_2$, and the reference signal is chosen $r(t) = [2\sin(0.02\pi t), 0]^T$. For a dwell time $\tau_d = 5$ sec, we pick $C = 1$ in (3-6) and the matrices obtained by solving the LMIs in (3-6), are:

$$P_{1,0} = \begin{bmatrix} 1.8426 & 0.0495 & -0.0142 & -0.5113 \\ 0.0495 & 0.2034 & -0.0064 & -0.0372 \\ -0.0142 & -0.0064 & 0.0193 & 0.0208 \\ -0.5113 & -0.0372 & 0.0208 & 0.9662 \end{bmatrix}$$

$$P_{1,1} = \begin{bmatrix} 2.5588 & 0.0174 & -0.0155 & -0.7376 \\ 0.0174 & 0.4338 & -0.0181 & -0.0097 \\ -0.0155 & -0.0181 & 0.0444 & 0.0251 \\ -0.7376 & -0.0097 & 0.0251 & 1.7162 \end{bmatrix}$$

$$P_{2,0} = \begin{bmatrix} 1.8612 & 0.0455 & -0.0108 & -0.5542 \\ 0.0455 & 0.2016 & -0.0062 & -0.0251 \\ -0.0108 & -0.0062 & 0.0182 & 0.0166 \\ -0.5542 & -0.0251 & 0.0166 & 1.0178 \end{bmatrix}$$

$$P_{2,1} = \begin{bmatrix} 2.5366 & 0.0283 & -0.0115 & -0.7328 \\ 0.0283 & 0.3913 & -0.0147 & -0.0110 \\ -0.0115 & -0.0147 & 0.0361 & 0.0197 \\ -0.7328 & -0.0110 & 0.0197 & 1.7429 \end{bmatrix}.$$

The parameters of the input quantizer $g_{\eta\mu}(u)$ in (2-8) are chosen as $M = 10$, $\Delta = 0.01$ and μ initially is equal to 1. The initial tracking error is $e(0) = [2, -1, 1, 0.5]^T$ and the initial parameter estimates are chosen

$$K_{\mathrm{x1}}(0) = \begin{bmatrix} -0.1899 & -0.1943 & 0.2210 & 0.3101 \\ -0.0142 & 0.0007 & -0.0014 & 0.0009 \end{bmatrix}^T, \; K_{\mathrm{r1}}(0) = 0.75 \cdot I_2$$

$$K_{\mathrm{x2}}(0) = \begin{bmatrix} -0.1853 & -0.1682 & 0.2238 & 0.3128 \\ -0.0138 & 0.0002 & -0.0012 & 0.0016] \end{bmatrix}^T, \; K_{\mathrm{r2}}(0) = 0.75 \cdot I_2.$$

The controller parameters are assumed to reside between lower and upper bounds as follows: $K_{\mathrm{r}p}^{(1,2)}, K_{\mathrm{r}p}^{(2,1)} \in [-1, 1]$, $K_{\mathrm{r}p}^{(1,1)}, K_{\mathrm{r}p}^{(2,2)} \in [0.5, 1.2]$ and $K_{\mathrm{x}p}^{(i,j)} \in [-1, 1]$, $i \in [1, 4]$, $j \in [1, 2]$, $p = 1, 2$ (the notation $K^{(i,j)}$ represents the (i, j)-th entry of matrix K). For the purpose of the simulation, Ω in (2-40) is computed $\Omega = 0.49$.

4-2-2 Simulation results

The simulation has been conducted in Matlab-Simulink® and the simulation results are shown in Figs. 4-10 – 4-14.

The switching sequence admissible with dwell time is shown in Fig. 4-10, while Fig. 4-11 shows the dynamic range μ. Fig. 4-12 shows that the tracking performance of the dynamic quantizer with adjustable offset is clearly satisfactory. From Fig. 4-11 it can be seen that the quantizer parameter μ retains its initial value for the initial 7 seconds indicating that the signal is not saturated; then it decreases abruptly in a piecewise manner indicating that the condition $e \in \mathscr{I}_2{}'(\mu)$ triggers (3-31) consecutively. Thereafter, because μ stays close to zero, we have from (2-10) that the quantized measurement of the input value $g_{\eta\mu}(u)$ is almost identical to the actual input value u, thus it holds $g_{\eta\mu}(u) \approx \eta = K_{\mathrm{x}p}^T x_{\mathrm{m}} + K_{\mathrm{r}p}$, $p \in \mathscr{N}$, which identifies with the desired input to achieve asymptotic tracking in the non-quantized switched systems model reference adaptive control case.

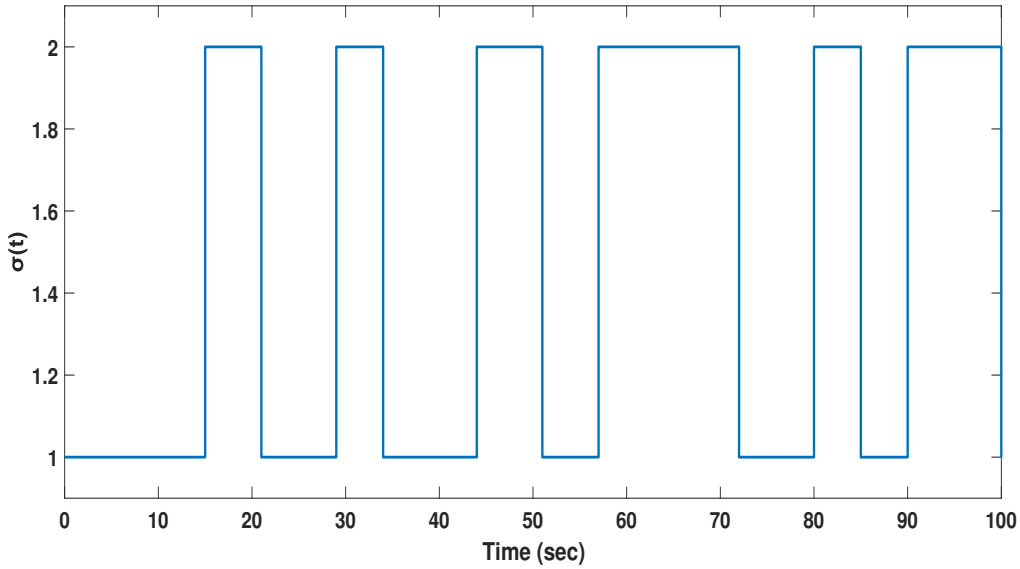

Figure 4-10: The switching signal $\sigma(t)$.

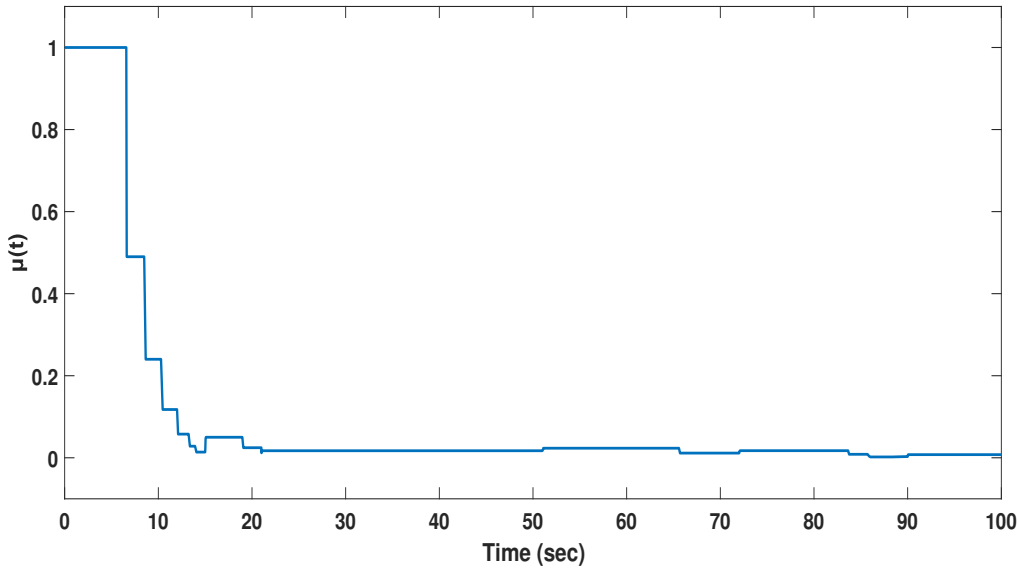

Figure 4-11: Hybrid control parameter $\mu(t)$.

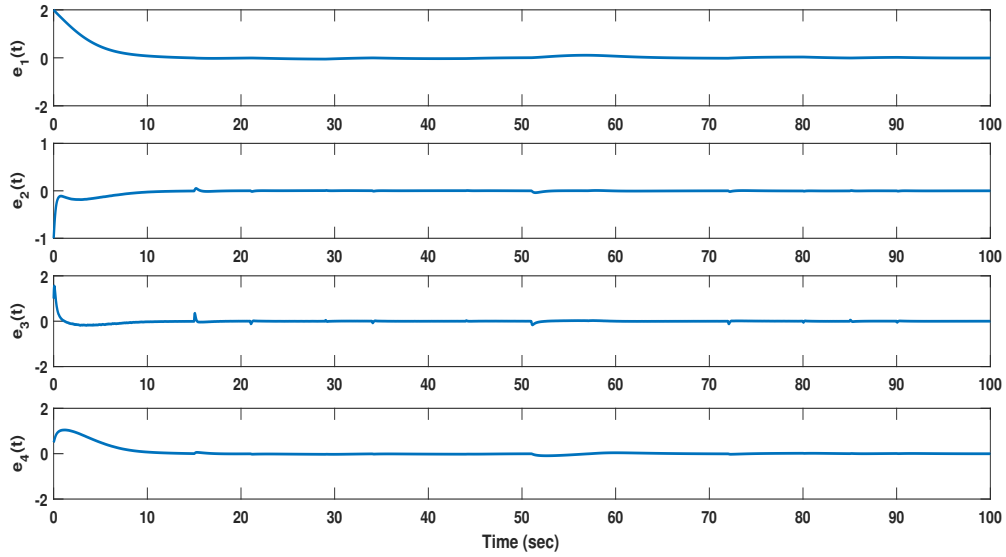

Figure 4-12: State tracking error

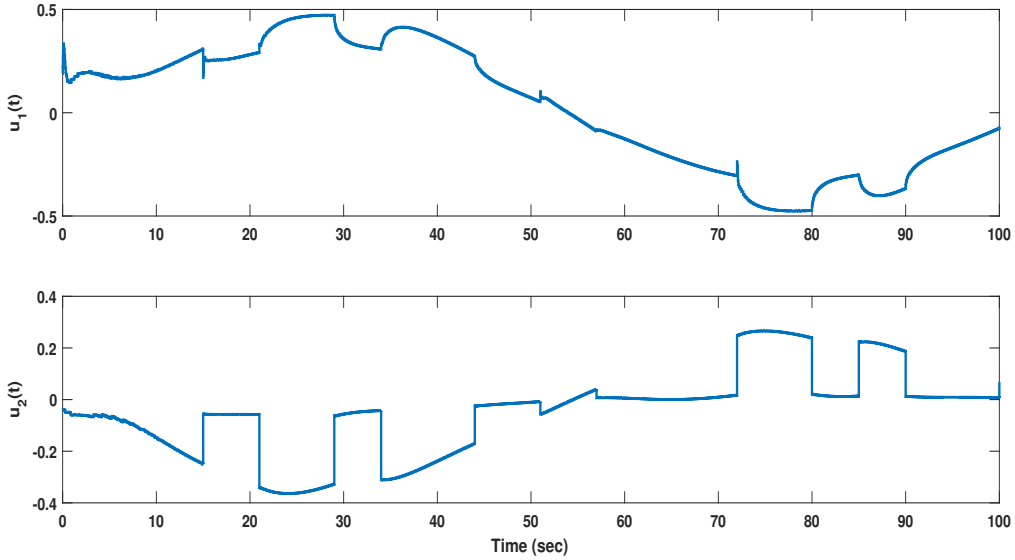

Figure 4-13: Quantized input

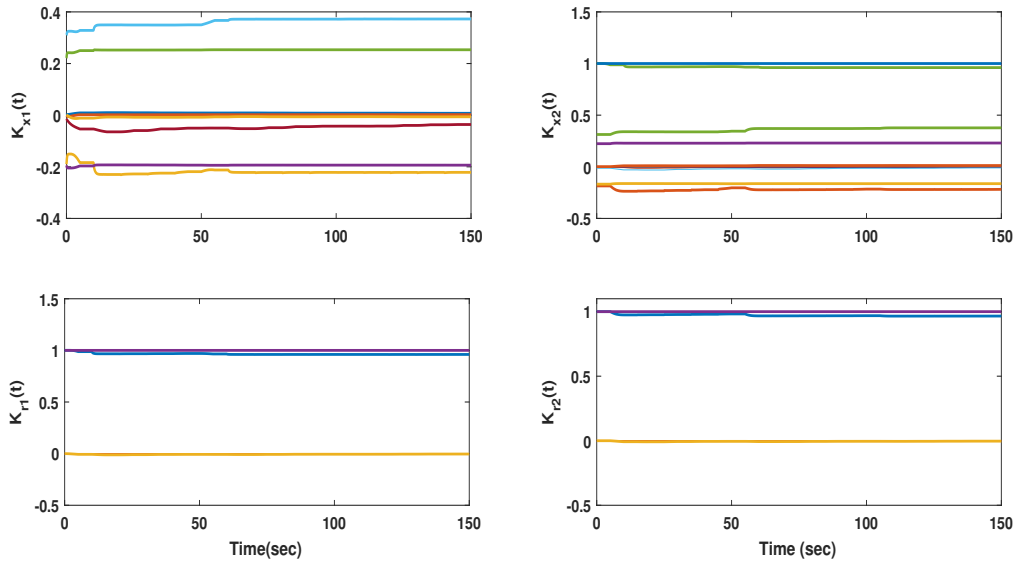

Figure 4-14: Controller parameter estimates

It can be seen in Fig. 4-11 that μ is not monotonically decreasing indicating zooming-out events in between zooming-in time intervals, which complies with our theoretical result in (3-30). When the condition $e \in \mathscr{B}_1{}'(\mu)$ tends to be violated, μ increases at a faster rate than the growth of $\|e\|$ to avoid saturation. It is important to underline that the zooming-out phases are mostly occurring in switching time instants, not in order to compensate the possible increment of the Lyapunov function at the switching instants (we have shown in (3-20) that this is not possible), but rather as a result of poor controller parameter estimates from the previous switch-out controller time instants. This is less evident, as the estimates settle for all subsystems, at 15s 51s, and 72s. Then μ decreases in a piecewise manner according to (2-40) when $e \in \mathscr{I}_2{}'(\mu)$, and subsequently smaller regions $\mathscr{I}_1{}'(\mu)$, $\mathscr{I}_2{}'(\mu)$ are obtained.

Chapter 5

Conclusions and future work

This Chapter concludes the MSc thesis. In Section 5-1 we recall the research questions from Section 1-3 and summarize how we tackled them. In Section 5-2, we formulate new research questions with a possible direction towards solving them.

5-1 Conclusions

The aim of this MSc thesis was to address the following aspects:

- *Address large uncertainty in the unknown system parameters*

  This was achieved by embedding quantized control in a model reference adaptive control framework.

- *Achieve asymptotic tracking in the quantized control setting, without sending information infinitely often*

  This was achieved by introducing a novel dynamic quantizer with dynamic offset. A Lyapunov-based approach was used to derive the adjustments of the dynamic range, of the dynamic offset, and of the control parameters.

- *Enlarge the class of quantized adaptive tracking control to include uncertain switched linear systems*

  We extended the quantized adaptive control scheme for switched linear systems with dwell-time switching, by exploiting a time-scheduling technique [53] to develop a new Lyapunov function with a time-varying positive definite matrix.

- *Avoid the quantizer to zoom out at every switching instants in order to compensate for discontinuities*

  Differently from the classic quadratic Lyapunov functions with a constant positive definite matrix, e.g. in [38] and [41], the new Lyapunov function is nonincreasing at the

switching instants, which does not require to zoom out at each switching instant. This mechanism greatly simplifies the design of the dynamic quantizer and makes it consistent with the zooming procedure in non-switched systems.

5-2 Future work

For the purposes of this Msc thesis we have implicitly assumed perfect, event-triggered, communication channels; once the control signal is available in the network, the quantized signal is directly transmitted to the unknown system. This framework does not take into account communication errors *(data-packet dropouts)*, which is the case in realistic networks [11]. In Chapter 3, the adaptive control of quantized-input switched linear systems under slow switching was investigated, assuming synchronous switching between each subsystem and its corresponding controller. This assumption is often unrealistic in practice [54]. Normally, because of the presence of the network closing the control loop, the controller switches later than the system which causes asynchronous switching in the closed-loop system. Apparently, the mismatched controller may lead to instability the closed-loop [55].

In Subsection 4-1-3, it was shown that asymptotic tracking can be achieved without infinite bandwidth. This was possible, because at each time instant only the bits that activate a new quantization level are transmitted through the network. An optimal dynamic bandwidth allocation management policy, which allocates the required bandwidth to guarantee asymptotic tracking for a certain bit rate could reduce the load of the network and save bandwidth for other components connected to the network.

From the above discussion, some new research questions are proposed as follows:

- Study the asymptotic tracking control for uncertain systems under communication losses, delays and quantization effect;
- Achieve asymptotic tracking for uncertain asynchronous switched systems;
- Design bandwidth allocation management policies in the framework of unknown systems with guaranteed asymptotic tracking.

In [56] a robust control approach is used, to evaluate the tracking performance taking into consideration network delays and data-packet dropouts. An LMI-based procedure is proposed for designing state-feedback controllers, which guarantee that the output of the closed-loop networked control system tracks the output of a given reference model in the H_∞ sense. A possible extension of this work, could be a hybrid control policy, similar to the one we used in Section 2.3, taking into account the quantization effect.

In [49], the stability problem for parametric uncertain switched systems in the presence of asynchronous dwell-time is addressed. A possible improvement to achieve asymptotic stability, could be the design of a new time-varying Lyapunov function, similar to the one we adopted in Section 3.2, with the difference that the new Lyapunov function is continuous at switching time instants and discontinuous at the instants when the system and controller modes are matched. If one can prove that the jumps of this Lyapunov function form a decreasing sequence then asymptotic stability is achieved.

A dynamic control-based approach to bandwidth management in NCSs has been proposed in [57]. In this work, each bandwidth allocation is determined locally for each loop, taking into account both the local plant dynamics and the global network dynamics. A possible extension to this work could be the expression of the error dynamics into an adaptive control framework using quantized measurements, and express the bandwidth allocation management policy taking into account the dynamics of the quantizer.

Appendix A

Preliminaries in stability for switched linear systems under time dependent switching

A-1 Time dependent switching

Suppose we are given a family of linear systems, $A_p \in \mathbb{R}^{n\times n}$, such that

$$\dot{x} = A_p x,\ p \in \mathscr{N} \tag{A-1}$$

where the index set $\mathscr{N}$ is finite: $\mathscr{N} = \{1, 2, ..., N\}$.

To define a switching signal generated by (A-1), we need the notion of a *switching signal*. This is a piecewise constant function $\sigma : [0, \infty) \to \mathscr{N}$. Such a function σ has a finite number of discontinuities, namely the *switching times*, on every interval between two consecutive switching times. The role of σ is to specify, at each time instant t, the index $\sigma(t) \in \mathscr{N}$ of the *active subsystem*, i.e., the system from the family (A-1) that is currently being followed. It is assumed that σ is continuous from the right everywhere: $\sigma(t) = \lim_{\tau \to t^+} \sigma(\tau)$, for each $\tau \geq 0$. An example of such a switching signal for the case $\mathscr{N} = \{1, 2\}$ is depicted in Fig. A-1.

A switched linear system with time-dependent switching can be described by the equation

$$\dot{x}(t) = A_{\sigma(t)} x(t),\ \sigma(t) \in \mathscr{N}. \tag{A-2}$$

A-1-1 Linear switched systems dwell-time stability

It is well known that a switched system with time-dependent switching is stable, if all individual subsystems in (A-1) are stable and the switching is sufficiently slow, so as to allow the transient effect to dissipate after each switching time instant. In this subsection, we discuss

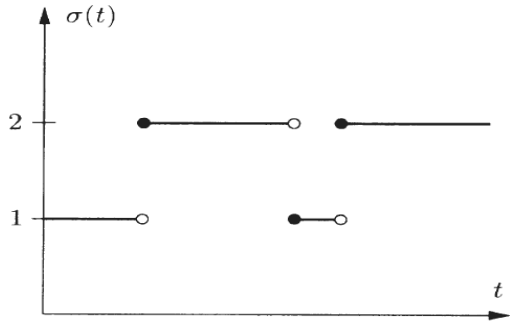

Figure A-1: A switching signal $\sigma(t)$ [2]

how this property can be precisely mathematically formulated and justified using multiple Lyapunov function techniques.

Lemma A-1.1. *[49]* ***(Dwell time global asymptotic stability)*** *Assume that each subsystem in (A-1) is globally asymptotically stable, that is, there exist positive definite matrices P_p and a constant scalar $\overline{\lambda} > 0$ such that the inequalities*

$$A_p^T P_p + P_p A_p + 2\overline{\lambda} P_p \leq 0,\ p \in \mathscr{N}, \tag{A-3}$$

hold. For a switching signal $\sigma(t)$, let t_i, $i \in \mathbb{N}^+$, denote the switching time instants and let τ_d represent the minimum switching time interval: $\tau_d = \min_{i \in \mathbb{N}^+}\{t_{i+1} - t_i\}$. By defining the following Lyapunov function candidate

$$V_{\sigma(t)}(x(t)) = x^T(t) P_{\sigma(t)} x(t) \tag{A-4}$$

for the switched linear system (A-1), the following properties are obtained:

1. *Each $V_p(x(t)) = x^T(t) P_p x(t)$ in (A-4) is positive definite, and its time derivative along the trajectory of the corresponding subsystem of (A-1) satisfies*

$$\begin{aligned} \dot{V}_p(t) &= x^T(t)(A_p^T P_p + P_p A_p)x(t) \\ &\leq -2\overline{\lambda} V_p(x(t)). \end{aligned} \tag{A-5}$$

2. *The inequalities*

$$\alpha_1 \|x(t)\|^2 \leq V_p(x(t)) \leq \alpha_2 \|x(t)\|^2 \tag{A-6}$$

   hold for $\alpha_1 = \min_{p \in \mathscr{N}}[\lambda_{min}(P_p)]$ and $\alpha_2 = \max_{p \in \mathscr{N}}[\lambda_{max}(P_p)]$.

3. *For $z = \frac{\alpha_2}{\alpha_1}$, it holds that*

$$V_p(x(t)) \leq z V_l(x(t)),\ \forall p, l \in \mathscr{N},\ p \neq l. \tag{A-7}$$

According to (A-5)-(A-7) and the result in [58], if the switching signal $\sigma(t)$ satisfies the dwell time condition

$$\tau_d \geq \frac{\ln z}{2\overline{\lambda}} \tag{A-8}$$

then the switched linear system (A-2) is globally asymptotically stable.

Remark 9. *If all A_p in (A-1) are the same, or there exists a common positive definite matrix P such that $A_p^T P + P A_p < 0$, the switched linear system (A-1) is globally asymptotically stable for arbitrary switching (arbitrary slow switching). Conditions for the existence of a common positive definite matrix P can be found in [59].*

Consider (A-1) with $\mathscr{N} = \{1, 2\}$ and let t_i, $i = 1, 2, ...$ be the switching instants. Let V_1 and V_2 given by (A-4) be their respective (radially unbounded) Lyapunov functions. In case a common P exists, the values of V_1 and V_2 coincide at each switching time, i.e., $V_{\sigma(t_{i-1})}(t_i) = V_{\sigma(t_i)}(t_i)$ for all i, and then V_σ is a continuous Lyapunov function for the switched system and asymptotic stability follows. This situation is depicted in Fig. A-2(a).

In case such common P does not exist, V_σ is discontinuous. While each V_p, $p \in \mathscr{N}$, decreases when the pth subsystem is active, it may increase when the pth subsystem is inactive. The idea that follows the dwell time property in Lemma A-1.1 is the following: by looking at the values of V_p at the beginning of each interval on which $\sigma = p$, the switched system (A-1) is globally asymptotically stable if these values form a decreasing sequence for each p. This situation is depicted in Fig. A-2(b).

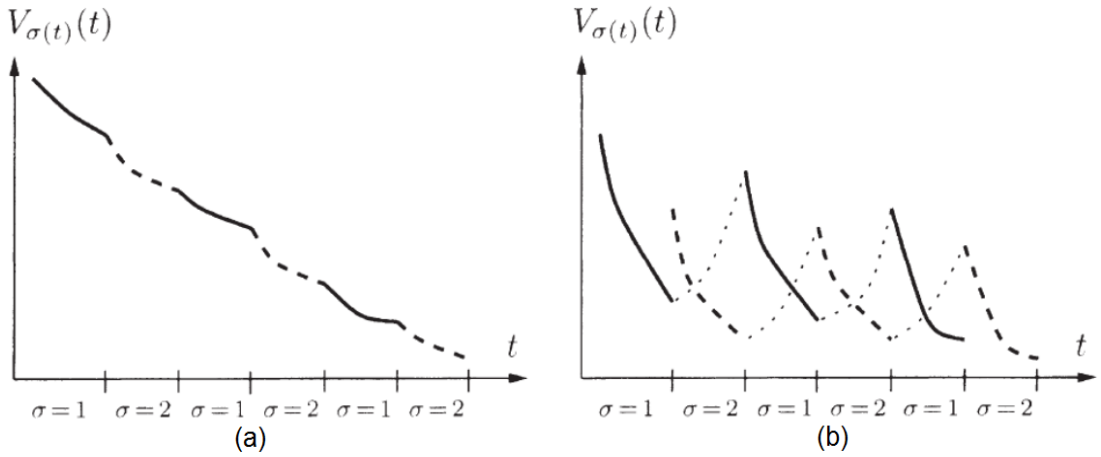

Figure A-2: Two Lyapunov functions (solid graphs correspond to V_1, dashed lines correspond to V_2): (a) continuous V_σ, (b) discontinuous V_σ [2]

Bibliography

[1] T. Yang. Networked control system: A brief survey. *IEEE Proceedings Control Theory and Applications*, 5:403 – 412, 2006.

[2] D. Liberzon. *Switching in systems and control*. Springer Science & Business Media, 2012.

[3] D. Liberzon. Quantized systems and control. DISC HS, 2003.

[4] G. Tao. *Adaptive control design and analysis*. John Wiley & Sons, 2003.

[5] K. S. Narendra and A. M. Annaswamy. *Stable adaptive systems*. Courier Corporation, 2012.

[6] S. Baldi, G. Battistelli, E. Mosca, and P. Tesi. Multi-model unfalsified adaptive switching supervisory control. *Automatica*, 46(2):249 – 259, 2010.

[7] K. S. Narendra and Z. Han. A new approach to adaptive control using multiple models. *International Journal of Adaptive Control and Signal Processing*, 26(8):778–799, 2012.

[8] N. E. Kahveci and P. A. Ioannou. Adaptive steering control for uncertain ship dynamics and stability analysis. *Automatica*, 49(3):685–697, 2013.

[9] J. Hu and W. X. Zheng. Adaptive tracking control of leader–follower systems with unknown dynamics and partial measurements. *Automatica*, 50(5):1416–1423, 2014.

[10] J. P. Hespanha, P. Naghshtabrizi, and Y. Xu. A survey of recent results in networked control systems. *Proceedings of the IEEE*, 95(1):138–162, 2007.

[11] L. Zhang, H. Gao, and O. Kaynak. Network-induced constraints in networked control systems—a survey. *IEEE Transactions on Industrial Informatics*, 9(1):403–416, 2013.

[12] F. Y. Wang and D. Liu. *Networked Control Systems: Theory and Applications*. Springer Publishing Company, Incorporated, 1st edition, 2008.

[13] R. W. Brockett and D. Liberzon. Quantized feedback stabilization of linear systems. *IEEE Transactions on Automatic Control*, 45(7):1279–1289, 2000.

[14] D. Liberzon. Hybrid feedback stabilization of systems with quantized signals. *Automatica*, 39(9):1543–1554, 2003.

[15] H. Ishii and B. A. Francis. Quadratic stabilization of sampled-data systems with quantization. *Automatica*, 39(10):1793–1800, 2003.

[16] A. Selivanov, A. Fradkov, and D. Liberzon. Adaptive control of passifiable linear systems with quantized measurements and bounded disturbances. *Systems & Control Letters*, 88:62–67, 2016.

[17] T. Hayakawa, H. Ishii, and K. Tsumura. Adaptive quantized control for linear uncertain discrete-time systems. *Automatica*, 45(3):692 – 700, 2009.

[18] T. Hayakawa, H. Ishii, and K. Tsumura. Adaptive quantized control for nonlinear uncertain systems. *Systems & Control Letters*, 58(9):625–632, 2009.

[19] J. Zhou, C. Wen, and G. Yang. Adaptive backstepping stabilization of nonlinear uncertain systems with quantized input signal. *IEEE Transactions on Automatic Control*, 59(2):460–464, 2014.

[20] Y. X. Li and G. H. Yang. Adaptive asymptotic tracking control of uncertain nonlinear systems with input quantization and actuator faults. *Automatica*, 72:177–185, 2016.

[21] G. Lai, Z. Liu, C. L. P. Chen, and Y. Zhang. Adaptive asymptotic tracking control of uncertain nonlinear system with input quantization. *Systems & Control Letters*, 96:23–29, 2016.

[22] K. Liu, Z. Ji, G. Xie, and L. Wang. Consensus for heterogeneous multi-agent systems under fixed and switching topologies. *Journal of the Franklin Institute*, 352(9):3670 – 3683, 2015. Special Issue on Synchronizability, Controllability and Observability of Networked Multi-Agent Systems.

[23] X. Xu and P. J. Antsaklis. Optimal control of switched systems based on parameterization of the switching instants. *IEEE Transactions on Automatic Control*, 49(1):2–16, 2004.

[24] S. Baldi, I. Michailidis, E. Ntampasi, B. Kosmatopoulos, I. Papamichail, and M. Papageorgiou. A simulation-based traffic signal control for congested urban traffic networks. *Transportation Science, Special Issue: Recent Advances in Urban Transportation Through Optimization and Analytics* , 2017.

[25] R. C. Loxton, K. L. Teo, V. Rehbock, and W. K. Ling. Optimal switching instants for a switched-capacitor dc/dc power converter. *Automatica* , 45(4):973 – 980, 2009.

[26] X. Q. Zhao and J. Zhao. Asynchronous fault detection for continuous-time switched delay systems. *Journal of the Franklin Institute*, 352(12):5915 – 5935, 2015.

[27] S. Tong, T. Wang, and Y. Li. Fuzzy adaptive actuator failure compensation control of uncertain stochastic nonlinear systems with unmodeled dynamics. *IEEE Transactions on Fuzzy Systems*, 22(3):563–574, 2014.

[28] R. Shorten, F. Wirth, O. Mason, K. Wulff, and C. King. Stability criteria for switched and hybrid systems. *SIAM Review*, 49(4):545–592, 2007.

[29] L. Zhang and H. Gao. Asynchronously switched control of switched linear systems with average dwell time. *Automatica* , 46(5):953 – 958, 2010.

[30] L. I. Allerhand and U. Shaked. Robust state-dependent switching of linear systems with dwell time. *IEEE Transactions on Automatic Control*, 58(4):994–1001, 2013.

[31] L. Zhang, S. Wang, H. R. Karimi, and A. Jasra. Robust finite-time control of switched linear systems and application to a class of servomechanism systems. *IEEE/ASME Transactions on Mechatronics*, 20(5):2476–2485, 2015.

[32] L. I. Allerhand and U. Shaked. Robust stability and stabilization of linear switched systems with dwell time. *IEEE Transactions on Automatic Control*, 56(2):381–386, 2011.

[33] S. Baldi and P. A. Ioannou. Stability margins in adaptive mixing control via a lyapunov-based switching criterion. *IEEE Transactions on Automatic Control*, 61(5):1194–1207, 2016.

[34] S. Yuan, B. De Schutter, and S. Baldi. Adaptive asymptotic tracking control of uncertain time-driven switched linear systems. *IEEE Transactions on Automatic Control*, pages to appear in 2017, available online.

[35] M. di Bernardo, U. Montanaro, and S. Santini. Hybrid model reference adaptive control of piecewise affine systems. *IEEE Transactions on Automatic Control*, 58(2):304–316, 2013.

[36] Q. Sang and G. Tao. Adaptive control of piecewise linear systems: the state tracking case. *IEEE Transactions on Automatic Control*, 57(2):522–528, 2012.

[37] S. Tong, Y. Li, and S. Sui. Adaptive fuzzy output feedback control for switched nonstrict-feedback nonlinear systems with input nonlinearities. *IEEE Transactions on Fuzzy Systems*, 24(6):1426–1440, 2016.

[38] M. Wakaiki and Y. Yamamoto. Quantized output feedback stabilization of switched linear systems. *In Proceedings of the 21st International Symposium on Mathematical Theory of Networks and Systems*, pages 758–763, 2014.

[39] R. Wang, J. Xing, J. Li, and Z. Xiang. Finite-time quantised feedback asynchronously switched control of sampled-data switched linear systems. *International Journal of Systems Science*, 47(14):3320–3335, 2016.

[40] J. Li and J. H. Park. Fault detection filter design for switched systems with quantization effects. *Journal of the Franklin Institute*, 353(11):2431 – 2450, 2016.

[41] M. Wakaiki and Y. Yamamoto. Stabilization of switched linear systems with quantized output and switching delays. *IEEE Transactions on Automatic Control*, 2017.

[42] G. Tao. Multivariable adaptive control: A survey. *Automatica*, (11):2737–2764, 2014.

[43] T. Wedi and S. Wittmann. Quantization offsets for video coding. In *IEEE International Symposium on Circuits and Systems*, pages 324–327, 2005.

[44] Q. Xu, X. Lu, Y. Liu, and C. Gomila. A fine rate control algorithm with adaptive rounding offsets (aro). *IEEE Transactions on Circuits and Systems for Video Technology*, 19(10):1424–1435, 2009.

[45] S. Notebaert, J. De Cock, K. Vermeirsch, P. Lambert, and R. Van de Walle. Leveraging the quantization offset for improved requantization transcoding of H.264/AVC video. In *2009 Picture Coding Symposium*, pages 1–4, 2009.

[46] V. Parameswaran, A. Kannur, and B. Li. Adapting quantization offset in multiple description coding for error resilient video transmission. *Journal of Visual Communication and Image Representation*, 20(7):491–503, 2009.

[47] Y. Su and J. Huang. Stability of a class of linear switching systems with applications to two consensus problems. In *Proceedings of the 2011 American Control Conference*, pages 1446–1451.

[48] M. Wakaiki and Y. Yamamoto. Output feedback stabilization of switched linear systems with limited information. In *IEEE 53rd Annual Conference on Decision and Control (CDC)*, pages 3892–3897, 2014.

[49] C. Wu, J. Zhao, and X. M. Sun. Adaptive tracking control for uncertain switched systems under asynchronous switching. *International Journal of Robust and Nonlinear Control*, (17):3457–3477, 2015.

[50] C. Wu and J. Zhao. H_∞ adaptive tracking control for switched systems based on an average dwell-time method. *International Journal of Systems Science*, 46(14):2547–2559, 2015.

[51] D. P. Stoten and S Bulut. Application of the mcs algorithm to the control of an electrohydraulic system. In *IECON, 20th International Conference on Industrial Electronics, Control and Instrumentation*, pages 1742–1747, 1994.

[52] Q. Sang and G. Tao. Multivariable adaptive piecewise linear control design for nasa generic transport model. *Journal of Guidance, Control, and Dynamics*, 35(5):1559–1567, 2012.

[53] W. Xiang. On equivalence of two stability criteria for continuous-time switched systems with dwell time constraint. *Automatica*, 54:36 – 40, 2015.

[54] Jian L. and G.H. Yang. Asynchronous fault detection filter design approach for discrete-time switched linear systems. *International Journal of robust and nonlinear control*, 24(1):70–96, 2014.

[55] Y. E. Wang, X. M. Sun, and J. Zhao. Stabilization of a class of switched stochastic systems with time delays under asynchronous switching. *Circuits, Systems, and Signal Processing*, 32(1):347–360, 2013.

[56] H. Gao and T. Chen. Network-based H_∞ output tracking control. *IEEE Transactions on Automatic Control*, 53(3):655–667, 2008.

[57] M. Velasco, J. M. Fuertes, C. Lin, P. Marti, and S. Brandt. A control approach to bandwidth management in networked control systems. *Industrial Electronics Society. IECON 2004, 30th Annual Conference of IEEE*, 3:2343 – 2348.

[58] J. P. Hespanha and A. S. Morse. Stability of switched systems with average dwell-time. In *Proceedings of the 38th IEEE Conference on Decision and Control*, pages 2655–2660, 1999.

[59] R. N. Shorten and K. S. Narendra. On the stability and existence of common lyapunov functions for stable linear switching systems. In *Proceedings of the 37th IEEE Conference on Decision and Control*, pages 3723–3724, 1998.